



# UNIVERSITÀ DI PARMA

## ARCHIVIO DELLA RICERCA

University of Parma Research Repository

Development, analysis and application of a predictive controller to a small-scale district heating system

This is the peer reviewed version of the following article:

*Original*

Development, analysis and application of a predictive controller to a small-scale district heating system / Saletti, C., Gambarotta, A., Morini, M.. - In: APPLIED THERMAL ENGINEERING. - ISSN 1359-4311. - 165:(2020), p. 114558. [10.1016/j.applthermaleng.2019.114558]

*Availability:*

This version is available at: 11381/2866075 since: 2023-05-29T12:57:10Z

*Publisher:*

Elsevier Ltd

*Published*

DOI:10.1016/j.applthermaleng.2019.114558

*Terms of use:*

Anyone can freely access the full text of works made available as "Open Access". Works made available

*Publisher copyright*

note finali coverpage

(Article begins on next page)

# Development, analysis and application of a predictive controller to a small-scale district heating system

Costanza Saletti<sup>a\*</sup>, Agostino Gambarotta<sup>a,b</sup>, Mirko Morini<sup>a,b</sup>

<sup>a</sup> *Department of Engineering and Architecture, University of Parma, Parco Area delle Scienze 181/A, 43124 Parma, Italy*

<sup>b</sup> *Center for Energy and Environment (CIDEA), University of Parma, Parco Area delle Scienze 42, 43124 Parma, Italy<sup>1</sup>*

---

## Abstract

District Heating and Cooling networks have great potential for energy saving, efficient thermal energy distribution and renewable energy source integration. Currently, heating systems are managed on the basis of operator experience or by using adaptive controllers, however these solutions are not suitable when there are remarkable variations in boundary conditions. In this context, Model Predictive Control is a promising strategy as it optimizes control based on the prediction of the future behavior of system dynamics and disturbances by means of simplified models. This paper presents the development of a predictive controller based on a novel Dynamic Programming optimization algorithm and aimed to supply the thermal energy to entire buildings within district heating networks. The controller is exploited to operate the district heating network of a school complex in a simulation environment (i.e. Model-in-the-Loop). Each branch connected to the network is optimized by a dedicated controller according to a multi-agent strategy. The performance of the innovative controller is compared to the results obtained by using a conventional PID controller. Conservative results show that, with the innovative controller, a reduction in fuel consumption of up to more than 7 % is obtained together with up to 5 hours of avoided failures of the indoor comfort constraints, depending on the season. Overall, the Model-based Predictive Controller is able to fulfill comfort requirements

---

\* Corresponding author.

E-mail address: [costanza.saletti@unipr.it](mailto:costanza.saletti@unipr.it)

adequately while minimizing energy consumption. Moreover, the multi-agent approach allows these results to be extended to larger networks in future studies.

*Keywords:* Model Predictive Control; Dynamic Programming; District Heating and Cooling network; identification; optimization.

---

## **1. Introduction**

Heating is the largest single energy end-use within buildings. It currently accounts for 42 EJ/yr, i.e. 36 % of the total building energy consumption [1]. Therefore, this large consumption must be taken as an opportunity to improve energy efficiency and to increase savings. A solution can be found from District Heating and Cooling networks (DHC) which, by distributing thermal energy to buildings (e.g. residential and commercial), give rise to synergies, such as gaining flexibility, increasing the share of renewable energy sources [2] and exploiting more energy efficient buildings [3].

At present, however, the large variety of available energy sources has introduced new challenges such as the efficient allocation of the load and the management of these systems [4]. Moreover, the high variability of weather conditions and atmospheric instability due, for instance, to climate change requires innovative approaches that are able to optimize energy distribution. In fact, the application of Smart Technologies is paramount in achieving the key targets (i.e. greenhouse gas emission reduction, energy efficiency improvement and production from renewables) established by the European Commission [5].

With this in mind, one of the most promising smart control strategies for energy systems is Model Predictive Control (MPC) which, contrary to conventional approaches, is based on the prediction of the future behavior of the system and external conditions (Figure 1). Model Predictive Control is a family of control strategies that uses a dynamic model of the system to predict its behavior over a future time horizon, named the prediction horizon. The dynamic behavior of the system and the

forecast of the external disturbances are exploited to calculate the optimal control law by solving a constrained optimization problem that minimizes cost function. The prediction horizon is discretized in a certain number of time-steps. The output of the MPC is a sequence of control actions that shall be executed to obtain the optimal behavior of the system. However, only the first element of this control law, corresponding to the first time-step, is actually implemented in the real system. Then, the time horizon is moved one step forward (i.e. receding time horizon strategy), the system state variables are updated with the measurements of their current values and the whole calculation is repeated. This state update produces implicit feedback and reduces the influence of the uncertainty of disturbances and modeling approximations.

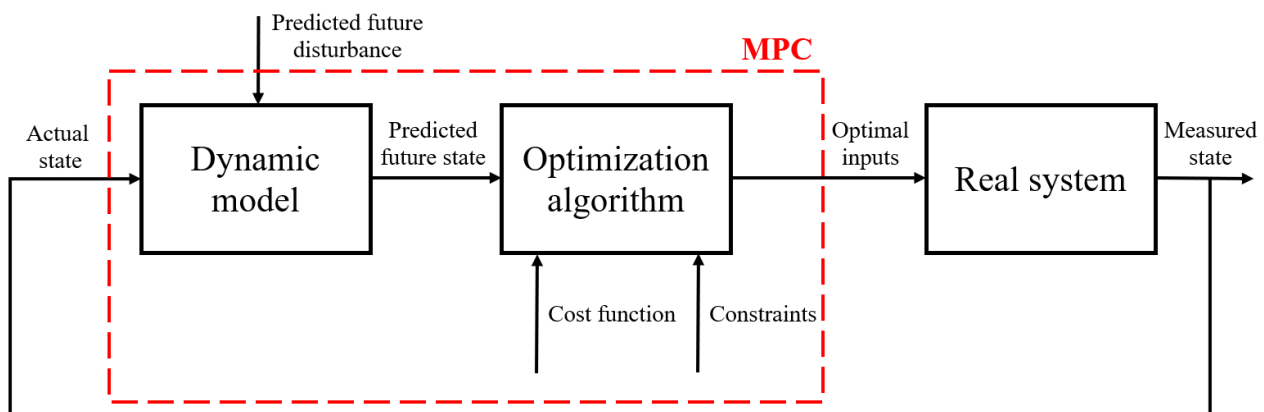


Figure 1. Schematic representation of the concept of Model Predictive Control: solution to a constrained optimization problem, which considers the prediction of the future behavior of the system by a dynamic model and the future disturbances. The resulting optimal inputs are used to control the system until the optimization problem at the following time-step is solved.

This control technique presents several advantages over other methods, such as [6]:

- it needs limited knowledge of control because its concepts are very intuitive;
- it can be used to control a large variety of processes;
- it can deal with multivariable cases;
- it introduces feed-forward control in a natural way to compensate for measurable disturbances.

Nevertheless, it presents some drawbacks, the most significant of which is the higher computational effort for the derivation of the control law with respect to traditional control methods. This has limited

the MPC applications to the areas in which the processes to be controlled are slow enough to enable online optimization [7]. The further developments in computing power and in modeling and optimization techniques have fostered the diffusion of MPC techniques, but it has to be underlined that the limit still remains: a balance has to be found between the complexity of the model of the controlled system and the necessity to obtain an optimal (or, in some cases, only feasible) control law within the length of a time-step. In any case, the prediction errors due to the simplifications in the model development are corrected by updating the system states by means of the measurements collected at each time-step. For this reason, black-box models identified on measurements or simplified white- or gray-box models are preferred to detailed physics-based models.

In this paper, an MPC controller is developed and analyzed. Detailed sensitivity analysis on the optimization algorithm parameters is performed in order to evaluate their influence on the algorithm accuracy and calculation time, which have to be suitable for MPC online implementation. Then, the MPC controller is tested through a Model-in the-Loop (MiL) platform. The case study is the thermal energy distribution grid of a school complex comprising two buildings and a boiler. A multi-agent approach is adopted for controlling the system. It consists of splitting the system into smaller subsystems optimized by dedicated agents. This allows the modular procedure to be verified, replicated and further implemented in more complex systems.

## **2. Literature review**

Model Predictive Control is one of the most recent control strategies that has been widely used in industry. The method was first introduced in the last decades of the 20th century [8], gaining relevant success mainly in the chemical and oil industries, as it introduced the possibility of controlling and simultaneously optimizing multi-variable processes subject to constraints, which are typical of this field [9]. Since then, a large number of theoretical results has been produced through control theory-

oriented research, providing a solid foundation for the technique concerning closed-loop stability [10], optimization algorithms [11], robustness and impact of stochastic disturbances [12].

In recent years, MPC has been applied in other fields such as: the control of Organic Rankine Cycles for the recovery of waste heat from the exhaust gases of automotive engines through a metaheuristic optimization algorithm [13] and through the comparison of two different MPC techniques [14]; solar thermal systems with borehole seasonal storage [15]; power control for domestic appliances [16]; hybrid transport refrigeration systems [17]; and radiant ceiling cooling systems through an experimental study [18]. These works show the benefits of MPC in terms of energy efficiency compared to classical methods and confirm that it is possible to address high variability in environmental and economic conditions.

The application of MPC in complex energy systems is more recent. In a detailed review on optimized control systems for energy management of building environments [19], a large number of research works is analyzed and compared. The control systems in buildings, which allow indoor comfort conditions to be achieved, are divided into two main groups:

- Conventional controllers, such as on/off switching controllers, proportional-integral-derivative (PID) controllers and adaptive controllers. PIDs are closed-loop feedback controllers which do not have any direct knowledge of the system and produce poor performance when used alone [20]. Adaptive controllers, instead, are able to self-regulate and adapt to the variations of the external conditions based on measured system signals;
- Intelligent controllers, such as learning methods (e.g. neural networks for the prediction of environmental parameters), model-based predictive control methods and agent-based control systems.

It is reported that, although the very first MPC implementations in building environments are recent (i.e. 2011 [21]), predictive controllers are becoming the more frequent strategies employed. As a matter of fact, conventional techniques rely on the knowledge of the past behavior of the system and do not consider the prediction of future conditions, while predictive controllers might be able to

overcome this limit. The most common computational optimization methods used in building energy research are also summarized. It is concluded that predictive systems should be developed and coupled to efficient optimization algorithms as well as other artificial intelligence techniques in order to overcome the potentially high computational costs. For instance, Killian and Kozek [22] answer ten relevant questions concerning the current status of MPC in building control. The main benefits of MPC (i.e. consideration of system dynamics, prediction of the disturbances, constraint handling and conflicting optimization goals) are highlighted together with the main challenges of its implementation. Other studies focus on MPC in the building automation for energy flexibility and efficiency and conclude that it outperforms most of the classical control techniques. In particular, Afram and Janabi-Sharifi [23] review the advantages and disadvantages of conventional controllers, hard controllers, soft controllers and hybrid controllers for the heating, ventilation and air conditioning (HVAC) systems dedicated to single buildings without considering potential applications to distributed systems. In a study by Clauß *et al.* [24], many papers that propose rule-based and optimal control strategies of building HVAC systems are analyzed according to energy flexibility key performance indicators. In another work [25], a model of an MPC with a linear state-space model is proposed for a single-zone residential application with a constant room temperature set for the whole year.

However, MPC controllers for building energy applications are not easy to develop [26] due to the need for a model that predicts the future behavior of the system and is accurate and also suitable for real-time optimization [27]. Ascione *et al.* [28] implement a highly detailed building model in EnergyPlus coupled with Matlab<sup>®</sup>, but the multi-objective optimization is performed daily by selecting a point on the Pareto front, which defines hourly values of the set-point temperatures for the building thermal zones. Similarly, Gholamibozanjani *et al.* [29] calculate the thermal demand offline by using EnergyPlus and an MPC which is dedicated to set-point tracking. In another study [30], the building model is based on an electrical equivalent (i.e. three resistances for each wall) for the heat transfer and moisture content but it is too detailed for real-time control. Moreover, it requires

information about the system that might not be directly available. Another approach involves machine learning techniques [31], such as artificial neural networks, to determine the indoor temperature and energy consumption of the building for given weather and occupancy conditions. This is combined with a genetic algorithm to optimize the temperature set-points [32]. The neural network is trained with simulation data but requires a parameter tuning procedure which is non-standard and highly problem-dependent. Furthermore, the algorithm is efficient only when the conditions comprised in the training dataset are verified and might not be reliable when highly variable external conditions occur.

Other works take into account multi-energy production systems. For instance, Bianchini *et al.* [33] demonstrate an MPC procedure suitable for a large building in a realistic simulation framework. A zone thermal model is exploited for the building energy demand prediction but the focus of the control strategy is the building HVAC system. Additionally, Sangi *et al.* [34] propose the real-life implementation of an exergy-based MPC with a linear model which is limited to a building HVAC system. On the other hand, an MPC based on a Mixed Integer Linear Programming (MILP) algorithm for a stand-alone building energy system consisting of multiple energy production and storage devices is presented by Fux *et al.* [35]. The MPC problem, however, is solved once a day and the building energy demand is obtained by considering typical load profiles instead of a detailed prediction model of the building thermal behavior, which might affect the operation significantly. Hence, despite the improved performance of the multi-source energy system, this energy management approach is not suitable for applications in distributed energy networks. A promising study proposes a distributed MPC algorithm applied to a combined thermal and electrical building energy system [36] which, however, has a high computational cost.

Despite the increasing interest that MPC is gaining in this context, however, implementation at district level (i.e. for the control of the energy supplied to a whole building) has not yet been sufficiently explored. Electrical distributed systems such as micro-grids [37] have received more attention compared to thermal networks. For instance, in a paper by Sultana *et al.* [38] a systematic review of

photo-voltaic and wind energy systems controlled by the MPC approach is presented but no other energy system is investigated.

Another broad overview of the literature on control strategies for unlocking flexibility and enhancing energy efficiency in thermal networks shows the status of current research [39]. The need for advanced controllers that are able to face the challenges imposed by the growing share of renewable energy sources and climate variable conditions is highlighted. Among the cited advanced technologies, there are predictive controllers and multi-agent systems which might be suitable to meet the requirements of robustness, efficiency and scalability for the controller of a thermal distribution network. Some recent examples of the MPC approach applied to district heating networks are mentioned below. Verrilli *et al.* [40] propose a model predictive controller that calculates the optimal operation of a district heating system with thermal energy storage based on the minimization of the cost of power generation. Although the novelty of this study can be found in the exploitation of the receding horizon approach in optimally scheduling energy production from multiple sources, the demand that must be met is not calculated through a physics-based model but with data-mining methods. On the other hand, in a work by Vanhoudt *et al.* [41], the building load of a small-scale district heating network is represented through the thermal-electrical analogy while the grid components are fitted to supplier data. Moreover, the optimization of the management of the system is performed based on operational costs, while the minimization of the primary energy consumption instead might increase further energy saving. Another robust control strategy based on MPC for a solar district heating network is analyzed by Lennermo *et al.* [42], but their study does not include the demand side. Long *et al.* [43] propose instead a versatile optimization-based management approach for multi-source energy systems that exploits the graph theory for the system representation and MPC for its control. Nonetheless, the dynamics of the buildings is not included in the analysis. Therefore, to the best of the authors' knowledge, there are no cases in which the optimization involves both the end-users, considered as dynamic physics-based models, and the distribution network in an integrated and unified approach.

The overview presented above underlines the necessity to conduct more research on the topic of MPC for district heating and cooling networks and complex energy systems, in order to fully explore its benefits and solve the current issues. In particular, there are three main drawbacks [22]: the need for (i) experts in the field of automatic control, (ii) modeling and (iii) controller design, especially for large and complex systems. These limits could be addressed by adopting a multi-agent technology, which allows a complex problem to be split into smaller subproblems that are solved by representative agents [19,44]. Hence, the development of a model-based predictive controller with an efficient optimization algorithm, which can be easily exploited to control generic thermal networks through a multi-agent strategy, might be helpful in reducing energy consumption for heating and cooling.

The above-mentioned works take advantage of various optimization algorithms: from mathematical programming (e.g. MILP), which can be computationally non-efficient when non-linear systems are involved or may require the tuning of the cost function weights [30], to heuristic techniques, which are highly parameter-dependent and do not guarantee the achievement of the global optimum [45]. Dynamic Programming (DP), on the other hand, is a sequential optimization method that has an exact optimization character and is used to solve energy operation optimization [46] or sizing problems [47]. This is exploited by Favre and Peuportier [48] to study the control of a low-energy building heating system but it is not suitable for multiple end-users and it is considered too computationally heavy for implementation in real controllers. Thus, the further investigation proposed in this work is beneficial for understanding the feasibility of the DP for district energy problems.

With reference to the limitations of the current status of scientific research outlined herein, the novelty of the contribution of this paper consists of:

- *A novel MPC specifically developed for district heating and cooling networks.* The most MPC in the literature are dedicated to the HVAC systems of single buildings [23,24,33,34], while the distribution network and its potentialities are not explored. For instance, the influence of the dynamics of the distribution network (e.g. time delays, network thermal capacity) on the operation can be analyzed only by addressing the system in its entirety. In other cases, the

production units are optimized without considering the end-users in the analysis [42,43]. In this work, the distribution and utilization units are coupled in a unified optimization framework and the MPC controls the distribution network by supplying the heat to the buildings by means of the building substation heat exchangers.

- *A deterministic building model* that does not require specific knowledge about the system (e.g. building configuration and properties) and is, therefore, readily extendable to the multiple end-users of a network. The typical models in the literature either are extremely detailed (e.g. thermal demand calculated offline [29]) or require a large dataset to be trained (e.g. artificial neural networks [31,32,40]). In this work, the model (i) represents the physical evolution of the building, (ii) can be identified with a small amount of data and (iii) is suitable for real-time optimal control.
- *A novel DP algorithm* that is computationally faster than those existing in the literature. Contrary to other works, in which the algorithm operates a daily calculation for scheduling due to the high complexity of the model [28–30,35], this approach allows the control actions to be updated every time-step (e.g. fifteen minutes) and, thus, is suitable for online optimization. In addition, the exploitation of this class of algorithms for energy application is still lacking in the literature.
- *A multi-agent strategy* suitable for the application of the controller in large distribution networks and different layouts in a modular way without (i) altering the system model or (ii) increasing the computational effort, which is often the cause for inapplicability in the existing literature studies.
- *The possibility to replicate this controller according to a fractal approach* (e.g. internal distribution of a single building, block of buildings, districts, etc), since the model has a general nature and, therefore, the problem can be extended to different scales.

### 3. Methods

In this paper, an MPC controller with a new optimization algorithm is developed and its performance is tested through an MiL platform and compared to that of a classical PID.

The sequence of operations followed in the controller development phase is represented in the block diagram in Figure 2 and illustrated in the following. In the first block, an optimization algorithm based on Dynamic Programming is developed and the algorithm parameters are analyzed through thorough sensitivity analysis. Then, a simplified dynamic system model for MPC implementation (i.e. MPC-model) is built and identified. The previously developed components are assembled in the MPC controller which aims to control real networks.

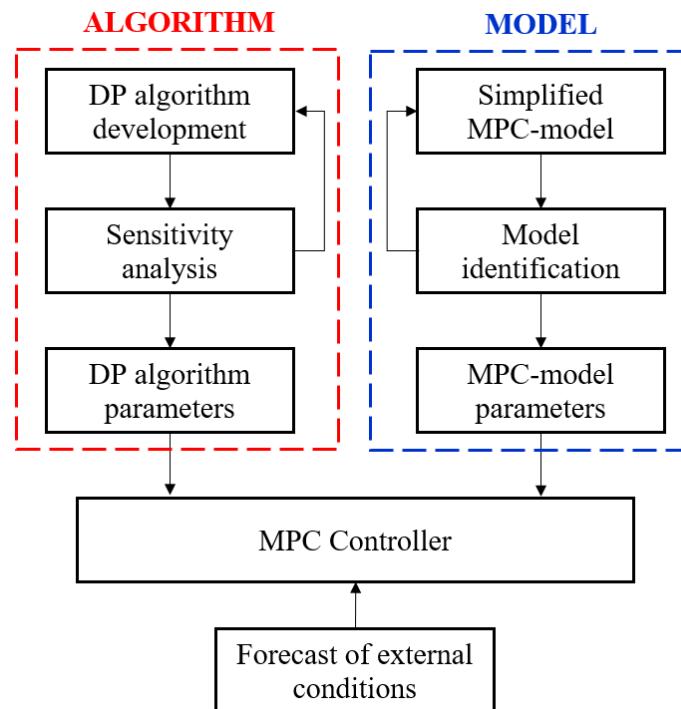


Figure 2. Block diagram of the method for the development of the innovative controller.

This section reports firstly the development of all the software components of the controller (i.e. models and algorithms), and secondly the development of the MiL application, which is used to test the control strategies in a simulation environment. In this way, the comparison can be performed in virtually equivalent boundary conditions and the controller development phase does not affect the operation of the real system.

### *3.1 Model Predictive Control development*

As explained in Section 1 and represented in Figure 1, Model-based Predictive Controllers are composed of: (i) a simplified dynamic model of the system, called the MPC-model, (ii) an optimization algorithm which solves the optimization problem and returns the optimal control trajectory, and (iii) a controller. The implementation of these elements in the Matlab<sup>®</sup> environment is discussed below.

#### *3.1.1 System model*

The system under consideration is the thermal distribution network of a school complex comprising two buildings (i.e. a school and a sports hall) and a boiler. Further applications will be possible starting from this test case. The most time-consuming part of the MPC implementation is generally the development of a suitable building model for control and operation, as a standard procedure does not exist, and each case should be evaluated separately [22].

When dealing with modeling heating distribution in buildings, different approaches can be used according to the characteristic scale on which the problem is investigated:

- on a micro-scale (e.g. when rooms or portions of buildings are of concern) a lot of information about the system (e.g. wall characteristics, glazed surface size and orientation) and about the disturbances (e.g. external temperatures, number and behavior of the occupants, other internal heat gain sources) can be accurately collected. Therefore, a dynamic detailed model of the system can be developed, which takes into consideration the building envelope characteristics and the forecast of internal gains and irradiance [25,30];
- on a macro-scale (e.g. when districts are of concern) less information is available for the characterization of the system. Dynamics, when considered, is limited to the main branches of the network [49] or to the storages [50] and users are mainly considered as stationary. Therefore, building heat demands are previously estimated through an historical data analysis

and then aggregated by means of statistical elaborations that consider contemporaneity factors [51];

- on a meso-scale, as is the case of this paper in which a network feeding blocks of buildings is considered, each building should be considered as a whole, therefore heat exchange and capacity properties are lumped together. Moreover, occupancy and the state of the glazed surfaces are difficult to estimate with an adequate accuracy for a whole building. Nevertheless, the building demand profile can be evaluated through a model that considers the influence of the main disturbance (e.g. external temperature).

The micro-scale problem is not addressed with a statistical approach, as historical data are rarely available in such detail or the instrumentation of small portions of buildings (zones) could be infeasible. On the other hand, in the macro-scale problem the detailed dynamics of the end-users can hardly be included due to the computational complexity of the system, that would become impracticable. The meso-scale problem, instead, makes it possible to benefit from the advantages of both the historical data, if available, and the knowledge of the physical system.

This is further confirmed by a comprehensive review of the recent efforts on building modeling methods for optimal control applications, which summarizes the three main model types that are typically implemented [52]:

- white-box models are based on detailed dynamic equations but their construction and solution process can be extremely time-consuming;
- black-box models are statistical models that require large datasets and long training periods. Their performance is acceptable when limited to the operating conditions they are trained for;
- gray-box models adopt a simplified description of the system but maintain a physical meaning of the parameters [53].

The third type seems to be advantageous for the application proposed in this work. As a matter of fact, the physics-based approach can efficiently simulate real system dynamics since it is based on conservation equations. Furthermore, a reduced-order gray-box model guarantees lower

computational effort, compared to more complex models. This is necessary for MPC online optimization, since the model has to be called a large number of times.

The simplified building model that is embedded in the MPC controller is derived from the building dynamic energy balance equation that describes the evolution of the internal temperature  $T$  [53] and is reported in Eq. (1):

$$\frac{dT}{dt} = -a \cdot (T - T_{\text{ext}}) + b \cdot \dot{Q} \quad (1)$$

where  $T_{\text{ext}}$  is the external ambient temperature and  $\dot{Q}$  is the thermal power supplied to the building substation heat exchanger and, then, distributed to the space heaters. The heat exchange through the walls to the external environment and the thermal power from the heating system influence the internal building temperature evolution through the coefficients  $a$  and  $b$ , respectively. These coefficients take into account the building heat capacity as reported by Gambarotta *et al.* [53]. As the MPC-model parameters  $a$  and  $b$  are unknown, an identification procedure has to be carried out from real building data. Forced ventilation is absent and air infiltrations are neglected. Moreover, internal and solar gains are not included in the MPC-model of Eq. (1) due to the need to adopt the previously highlighted simplifications. More details on this choice can be found in Section 3.1.2.

A schematic representation of the distribution pipeline for each end-user with the relevant pipe sections highlighted is given in Figure 3. The purpose of the simplified representation of this part of the system is to give an immediate view of the nomenclature (equations and variables) used in the following. The thermal power given to the building is expressed as the variation in water enthalpy through the building substation heat exchanger as in Eq. (2):

$$\dot{Q} = \dot{m} \cdot c \cdot (T_S - T_{R,SP}) \quad (2)$$

where  $\dot{m}$  is the water mass flow rate,  $c$  is the water specific heat capacity,  $T_S$  and  $T_{R,SP}$  are the supply (i.e. to the heat exchanger) and return (i.e. from the heat exchanger) water temperature, respectively.

The return water temperature  $T_{R,SP}$  is a boundary condition for this simplified model, according to the assumption that it is regulated by the substation heat exchanger controller. Hence, it is set at a

given set-point value. The thermal power is transferred from the boiler to the building substation heat exchanger through the distribution pipes, which are located underground. A mixing valve recirculates a part of the return water to regulate the mixing temperature.

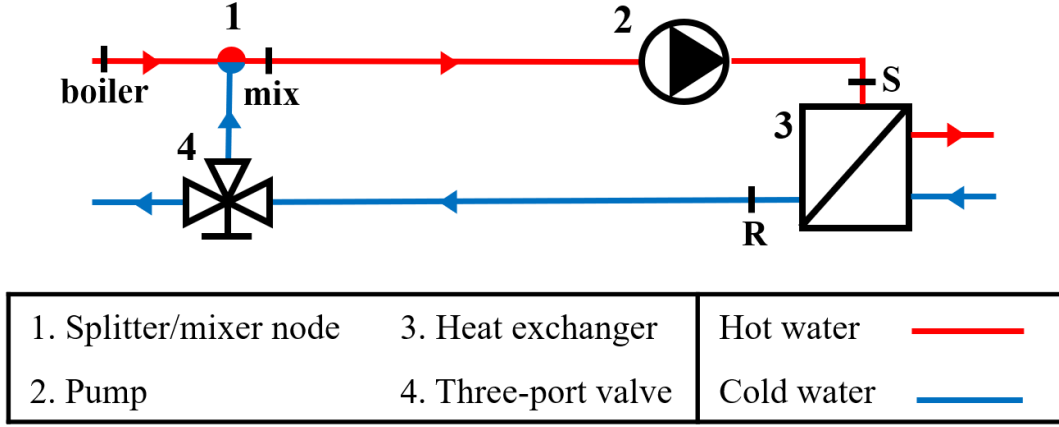


Figure 3. Schematic representation of the distribution pipeline for each building. Pipe sections are defined as follows: **boiler**: boiler; **mix**: mixing; **S**: supply; **R**: return.

Hence, the actual supply temperature  $T_S$  can be calculated by starting from the mixing temperature  $T_{\text{mix,SP}}$  and considering the heat losses of the supply pipe  $\dot{Q}_{\text{loss,S}}$ , as in Eqs. (3) and (4). The heat losses of the return pipe  $\dot{Q}_{\text{loss,R}}$  are given by Eq. (5):

$$T_S = T_{\text{mix,SP}} - \frac{\dot{Q}_{\text{loss,S}}}{\dot{m} \cdot c} \quad (3)$$

$$\dot{Q}_{\text{loss,S}} = UA \cdot (T_{\text{mix,SP}} - T_{\text{soil}}) \quad (4)$$

$$\dot{Q}_{\text{loss,R}} = UA \cdot (T_{\text{R,SP}} - T_{\text{soil}}) \quad (5)$$

where  $UA$  is the overall heat transfer coefficient, including the heat transfer surface, from the water in the pipes to the soil. The heat losses are calculated with respect to the highest temperatures, i.e.  $T_{\text{mix,SP}}$  for the supply pipe and  $T_{\text{R,SP}}$  for the return pipe, in order to have a conservative estimation.

The internal building temperature  $T$  is the system state and controlled variable of each building. The water mass flow rate  $\dot{m}$  and the set-point for the mixing temperature  $T_{\text{mix,SP}}$  are the manipulated variables of each building (i.e. inputs).

The boiler power is given by Eq. (6), which considers the sum of the heat transferred to the building substation heat exchangers of the network from Eq. (2) and the heat losses of the supply and return pipe from Eqs. (4) and (5):

$$P_{\text{boiler}} = \sum \left[ \dot{m} \cdot c \cdot (T_S - T_{R,SP}) + \dot{Q}_{\text{loss,S}} + \dot{Q}_{\text{loss,R}} \right] \frac{1}{\eta_{\text{boiler}}} \quad (6)$$

where  $\eta_{\text{boiler}}$  is the boiler efficiency, which is subject to a linear correction with the actual load with respect to the nominal efficiency.

The pump power is proportional with a constant coefficient  $k$  to the cube power of the water mass flow rate as in Eq. (7), which is derived from the expression of the distributed pressure losses through the pipes (i.e. Darcy-Weisbach equation).

$$P_{\text{pump}} = \sum \left[ \frac{8fL}{\pi^2 \rho^2 D^5} \cdot \frac{1}{\eta_{\text{pump}}} \cdot \dot{m}^3 \right] = \sum k \cdot \dot{m}^3 \quad (7)$$

where  $f$  is the friction factor,  $L$  is the pipe length,  $\rho$  is the water density,  $D$  is the pipe diameter and  $\eta_{\text{pump}}$  is the pump efficiency.

### 3.1.2 Forecasting of external data

Predictive controllers take advantage of their capability to optimally operate the system relying on the forecast of the disturbances throughout the prediction horizon. When dealing with real applications, the external ambient temperature, which is the main disturbance, can be collected by querying real-time weather forecast databases. In this work, this database is created through a piecewise function that reasonably builds the temperature profile using the maximum and minimum temperatures of the current day, the minimum temperature of the following day and the sunrise and sunset hours [54].

Solar radiation and internal gains due to the building occupancy are other disturbances of these systems. However, when dealing with a whole building it is not possible to have an accurate estimation of the contribution of building occupation and radiation, since the former depends on the

actual number of occupants and the latter depends on the shading of each single glazed surface. In the MPC-model described in Section 3.1.1, these contributions can be added, if available, but are not strictly required. In this application, they are also neglected to show the feasibility and robustness of the controller even when less knowledge about the system is obtainable, since the simplicity of the model is an advantage when extending this study to large networks. This assumption is commonly made in many other studies in the literature, where DHC networks are involved [51].

### *3.1.3 Optimization algorithm*

Within the MPC framework, an optimization problem has to be solved at each time-step (i.e. minimization/maximization of the cost function). Therefore, an optimization algorithm that combines low computational time with feasible accuracy had to be chosen. The Dynamic Programming algorithm is selected since it has an exact and inherently dynamic optimization character, as reported in Section 2.

The Dynamic Programming algorithm is based on Bellmann's principle of optimality which states that the tail of an optimal trajectory of an optimization problem is still optimal for the tail subproblem. According to this concept, the time scale and the whole state-space of an optimization problem are discretized and the global problem is divided into smaller subproblems that are solved recursively by proceeding backward in the time scale. During this time-backward calculation, for each step of the algorithm (i.e. subproblem) the state function and the related value of the cost function are evaluated for each feasible combination of the state and input grids. At each time-step, the inputs that minimize the cumulative cost, from the current step to the end of the prediction horizon, for each feasible state are stored in the memory. The procedure covers the entire prediction horizon and allows the dynamics of the system to be included in the optimization. Hence, this iterative calculation returns an optimal control map which is then exploited to identify the optimal control sequence through a forward calculation that starts from the initial condition.

In Sundström and Guzzella’s research [55], a Matlab<sup>®</sup> function, which solves generic DP problems with up to five state variables, has been proposed and is widely used in several applications (e.g. [56]). In this work, a novel and simpler function based on the same concept is developed in Matlab<sup>®</sup> and is designed to more efficiently handle the presented application and other problems with the same structure, i.e. one state (e.g. internal building temperature), two inputs (e.g. water mass flow rate and boiler temperature) and the disturbances (e.g. external temperature). This approach significantly simplifies multi-agent implementation, as the application of the controller to the different buildings can be operated in a modular way easily by changing each building model data and parameters. The novel function takes approximately one quarter of the time requested in [55] to solve the same optimization problem and allows a variable-step state/input discretization (e.g. local grid refinement). As the DP algorithm requires the discretization of the state and input grids, the MPC-model of the energy system in this application is obtained by discretizing Eq. (1). The discretized state equation at the  $k$ -th time-step (i.e.  $\Delta t$ ) is represented in Eq. (8):

$$\frac{T_{k+1} - T_k}{\Delta t} = -a \cdot (T_k - T_{\text{ext}}) + b \cdot \dot{Q} \quad (8)$$

By renaming the state  $T$  with  $x$ , the input  $\dot{m}$  with  $u_1$ , the input  $T_{\text{mix,SP}}$  with  $u_2$  and the disturbances  $T_{\text{ext}}$  and  $T_{\text{soil}}$  with  $d_1$  and  $d_2$ , respectively, and by considering Eqs. (2–5), Eq. (9) is obtained:

$$x_{k+1} = (1 - \Delta t \cdot a)x_k + \Delta t \cdot a \cdot d_{1,k} + \Delta t \cdot b \cdot (cu_{1,k}u_{2,k} - UA(u_{2,k} - d_{2,k}) - cu_{1,k}T_{R,SP}) \quad (9)$$

The input grid is created according to the lower and upper constraints of the input variables. The state grid is discretized according to the state boundary values. The steps of the input and state grids are algorithm parameters that can be set according to the sensitivity analysis described in Section 4.

The cost function for each time-step in Eq. (10) is assumed as the total energy consumption, consisting of the sum of the boiler energy and the pump energy (see Eqs. (6–7) respectively):

$$\text{cost} = (P_{\text{boiler}} + P_{\text{pump}}) \cdot \Delta t + \varphi \quad (10)$$

When the building is occupied, the internal temperature is constrained according to the lower and upper limits established by the contracts for service-sector buildings. Otherwise, the building

temperature is not constrained. The penalty factor  $\varphi$  is therefore added to the cost function associated with the unacceptable state values in order to force compliance with the constraints. The DP algorithm linearly increases the penalty factor as the distance from the state constraints increases, until the maximum penalty value is reached.

#### *3.1.4 Time delays*

It is necessary to consider pipe dynamics in the simulation and optimization of DHC networks [57]. As a matter of fact, the thermal energy that is generated at the production sites is distributed to the utilization sites that can be significantly far away, especially in large networks, and the time delay between production and effective supply to buildings might affect the operation and control of the system. Moreover, the thermal capacity of distribution pipes could be exploited as thermal storage by adopting different management strategies. Various studies in the literature present thermo-hydraulic pipe models (e.g. the plug-flow method) that are typically used in detailed dynamic simulations [58]. However, MPC implementation requires a simplified model that can be used to predict the future behavior of the system at each time-step. Furthermore, the pipe dynamics would require the introduction of an additional system state variable, however, this is not in line with the structure of the DP algorithm.

In this work, the MPC-model considers the time delays by introducing a factor  $\Delta t_d$ , for each calculation. This is defined as the ratio between the pipe length and the current speed (calculated from the current mass flow rate), and represents the delay with which the water mass flow reaches the building. The DP algorithm gives the optimal mixing temperature. In the current time-step, however, the temperature of the water that actually reaches the building remains at the same temperature as the previous time-step for a time interval equal to  $\Delta t_d$ . Hence, the optimal mixing temperature is increased in order to send the same amount of energy required for the current time-step, as in Eq. (11):

$$T_{\text{new}} = \frac{T_{\text{DP}} \cdot \Delta t - T_{\text{previous}} \cdot \Delta t_d}{\Delta t - \Delta t_d} \quad (11)$$

where  $T_{\text{new}}$ ,  $T_{\text{DP}}$  and  $T_{\text{previous}}$  are the new input, the optimal DP input and the previous time-step input, respectively.

This solution guarantees that the model structure is maintained and that the energy requirements of the users are respected. Equation (11) is valid when  $\Delta t_d < \Delta t$ , which represents the condition of the case study of this work. In other cases, different strategies can be adopted to consider time delays.

### 3.2 Model-in-the-loop platform

This section reports the description of the architecture of the MiL application platform, which is used to test different control strategies in a simulation environment. The MiL is a testing technique for control units in the development phase, in which they are emulated by specific models: hence, a model of the control device controls a model of the system in a virtual environment. The MiL approach allows methodologies to be tested and sensitivity analysis to be performed without involving the real system which could be unavailable due to the non-heating season or the need to respect building comfort conditions.

In order to simulate real building behavior, a detailed continuous-time dynamic model of the system, named the MiL-model, is used.

As introduced in Section 3.1.4, the distribution system dynamics cannot be neglected. Therefore, the MiL-model of each utilization site comprises the building model and the distribution network thermal model. The distribution network includes, for each end-user, the supply pipe, substation heat exchanger, return pipe and three-port recirculation valve, as in Figure 3.

The pipe model is built with a lumped parameter approach, according to which it is assumed that the water mass inside the pipe is at the same temperature ( $T_{\text{pipe,S}}$  for the supply,  $T_{\text{pipe,R}}$  for the return). It is possible to write the thermal energy balance of the supply pipe as in Eq. (12a), where the inflowing

fluid is at the mixing temperature while the outflowing fluid (i.e. water sent to the building substation heat exchanger) is at the supply pipe temperature  $T_{\text{pipe,S}}$ .

The building MiL-model is based on Eq. (1). In this case, the contributions of solar irradiance  $\dot{Q}_{\text{irr}}$  and thermal power from building occupation  $\dot{Q}_{\text{occ}}$  are assumed to be known, as this model aims to simulate the actual behavior of the real system. Hence, they are imposed as disturbances to obtain Eq. (12b). Similarly to the supply side, the thermal energy balance of the return pipe is expressed in Eq. (12c), where the inflowing fluid is at the actual return temperature from the building substation heat exchanger  $T_{\text{R}}$  while the outflowing fluid (i.e. water sent to the return collector and then to the boiler) is at the return pipe temperature  $T_{\text{pipe,R}}$ . A system of three ordinary differential equations is obtained:

$$\frac{dT_{\text{pipe,S}}}{dt} = \frac{1}{Mc} \cdot [\dot{m} \cdot c \cdot (T_{\text{mix}} - T_{\text{pipe,S}}) - UA \cdot (T_{\text{pipe,S}} - T_{\text{soil}})] \quad (12a)$$

$$\frac{dT}{dt} = -\tilde{a} \cdot (T - \hat{T}_{\text{ext}}) + \tilde{b} \cdot [\dot{m} \cdot c \cdot (T_{\text{pipe,S}} - T_{\text{R}}) + \dot{Q}_{\text{irr}} + \dot{Q}_{\text{occ}}] \quad (12b)$$

$$\frac{dT_{\text{pipe,R}}}{dt} = \frac{1}{Mc} \cdot [\dot{m} \cdot c \cdot (T_{\text{R}} - T_{\text{pipe,R}}) - UA \cdot (T_{\text{pipe,R}} - T_{\text{soil}})] \quad (12c)$$

where  $M$  is the mass of the water contained in the pipe and  $\tilde{a}$  and  $\tilde{b}$  are the performance coefficients of the real building. The external temperature profile  $\hat{T}_{\text{ext}}$  described previously is randomly altered in order to account for weather variability.

Unlike the MPC-model described in Section 3.1.1, the actual temperature of the return water from the substation heat exchanger  $T_{\text{R}}$  is calculated by means of the thermal energy balance of the substation heat exchanger as in Eq. (13), in which the heat is entirely transferred from the water in the primary side (i.e. distribution network) to the water in the secondary side (i.e. distribution to the building space heaters):

$$\dot{m} \cdot c \cdot (T_{\text{pipe,S}} - T_{\text{R}}) = \dot{m}_{\text{sec}} \cdot c \cdot \Delta T_{\text{sec}} \quad (13)$$

where  $\dot{m}_{\text{sec}}$  and  $\Delta T_{\text{sec}}$  are the water mass flow rate and temperature difference, respectively, on the secondary side of the substation heat exchanger. It is assumed that, given the design temperature

difference on the secondary side, a proportional feedback controller varies the water mass flow rate on the secondary side in order to maintain the set-point return temperature on the primary side  $T_{R,SP}$ .

The proportional law is given in Eq. (14):

$$\dot{m}_{sec} = K_{p,sec}(T_R - T_{R,SP}) \quad (13)$$

where  $K_{p,sec}$  is the proportionality constant. Hence, considering Eqs. (13) and (14), it is possible to obtain  $T_R$  through Eq. (15):

$$T_R = \frac{\dot{m}T_{pipe,S} + K_{p,sec}T_{R,SP}\Delta T_{sec}}{\dot{m} + K_{p,sec}\Delta T_{sec}} \quad (15)$$

Proceeding on the return side of the distribution network, a feed-forward controller regulates the mass flow rate that is recirculated from the return to the supply pipe by means of the three-port valve (Figure 3) in order to maintain the mixing temperature indicated by the MPC. The recirculated mass flow rate  $\dot{m}_{rec}$  is expressed by Eq. (16):

$$\dot{m}_{rec} = \frac{T_{boiler,SP} - T_{mix}}{T_{boiler,SP} - T_{R,SP}} \cdot \dot{m} \quad (16)$$

where  $T_{boiler,SP}$  is the set-point for the water that exits the boiler, chosen as the maximum of the optimal mixing temperature calculated by the MPC controllers of the end-users connected to the network. Indeed, the boiler controller keeps this maximum desired water temperature, while the water temperature effectively sent to each end-user is kept by regulating the recirculated mass flow rate, as explained previously.

The returning mass flows from each end-user are mixed in the return collector and conveyed back to the boiler. Therefore, the boiler mass flow rate  $\dot{m}_{boiler}$  and return temperature  $T_{boiler,R}$  are evaluated through the mass and energy balance equations of the return collector according to Eqs. (17):

$$\dot{m}_{boiler} = \sum_i (\dot{m}_i - \dot{m}_{rec,i}) \quad (17a)$$

$$T_{boiler,R} = \sum_i \frac{(\dot{m}_i - \dot{m}_{rec,i})T_{pipe,R,i}}{\dot{m}_{boiler}} \quad (17b)$$

The thermal model of the distribution network also includes the boiler, which is a standard boiler powered by natural gas. It is controlled by regulating the fuel mass flow rate  $\dot{m}_f$  in order to guarantee the set-point  $T_{\text{boiler,SP}}$  according to the feedback proportionality law in Eq. (18):

$$\dot{m}_f = K_{p,f}(T_{\text{boiler,SP}} - T_{\text{boiler}}) \quad (18)$$

where  $K_{p,f}$  is the proportionality constant and  $T_{\text{boiler}}$  is the actual temperature of the fluid exiting the boiler. The latter can be calculated by combining Eq. (18) with Eqs. (19), which represent the thermal power  $\dot{Q}_{\text{boiler}}$  of the boiler and its efficiency  $\eta_{\text{boiler}}$ :

$$\dot{Q}_{\text{boiler}} = \dot{m}_f \cdot LHV \cdot \eta_{\text{boiler}} = \dot{m}_{\text{boiler}} \cdot c \cdot (T_{\text{boiler}} - T_{\text{boiler,R}}) \quad (19a)$$

$$\eta_{\text{boiler}} = \frac{\dot{Q}_{\text{boiler}} - \dot{Q}_{\text{min}}}{\dot{Q}_{\text{nom}} - \dot{Q}_{\text{min}}}(\eta_{\text{nom}} - \eta_{\text{min}}) + \eta_{\text{min}} \quad (19b)$$

where  $LHV$  is the fuel lower heating value,  $\dot{Q}_{\text{nom}}$ ,  $\dot{Q}_{\text{min}}$ ,  $\eta_{\text{nom}}$  and  $\eta_{\text{min}}$  are the nominal and minimum power and the nominal and minimum efficiency, respectively, according to the linear correction with the actual boiler load. In light of these equations, the actual boiler temperature is obtained by Eq. (20):

$$T_{\text{boiler}} = \frac{\dot{m}_{\text{boiler}} \cdot c \cdot T_{\text{boiler,R}} + K_{p,f} \cdot LHV \cdot \eta_{\text{boiler}} \cdot T_{\text{boiler,SP}}}{\dot{m}_{\text{boiler}} \cdot c + K_{p,f} \cdot LHV \cdot \eta_{\text{boiler}}} \quad (20)$$

Since the calculations of the actual boiler temperature and thermal power are coupled, Eqs. (19) and (20) are solved through an iteration loop embedded in the global MiL-model.

The system of differential equations (12), which describe the dynamic behavior of the main components of each branch of a DHC system (i.e. building and pipes), are solved through a Matlab<sup>®</sup> Ordinary Differential Equation solver. The MiL-model runs continuously for the desired time span and is controlled by a model of the controller. Two different controllers are implemented and compared: (i) a state-of-the-art PID controller [53], the set-point of which comes into effect at an arbitrary point in time prior to occupation of the building (three hours) and (ii) the MPC controller described above. In the latter case, the optimal inputs calculated by the MPC controller of each end-user are given to the MiL-model as the mass flow rate  $\dot{m}$  and the mixing temperature  $T_{\text{mix}}$ .

#### 4 Sensitivity analysis

The DP algorithm that solves the constrained optimization problems at each time-step of the MPC implementation has been described in Section 3.1.3. However, the DP algorithm requires the discretization of the state and input grids and the choice of the parameters might affect the algorithm performance. Therefore, detailed sensitivity analysis of the characteristic parameters of the algorithm is presented in this section.

The lower and upper constraints of the input grid are established in the data definition phase and they typically represent the physical boundaries of the input signals (i.e. minimum and maximum mass flow rate and minimum and maximum mixing temperature). Similarly, the state grid boundary values define a plausible range of variation in the internal building temperature, which is set between 0 °C and 30 °C in this application. The time-step is 15 min, which is reasonable for thermal energy applications. The time horizon is three days.

The sensitivity analysis is conducted by varying the state grid steps (i.e.  $\Delta x$ ) and the input grid steps (i.e.  $\Delta u_1$  and  $\Delta u_2$ ) independently and by comparing the performance of the algorithm according to some key performance indicators, which are selected as follows:

- Computational time for a single DP algorithm calculation;
- Predicted global energy consumption over the time horizon of a single DP algorithm calculation;
- The number of time-steps in which the compliance with the temperature constraints is not realized (i.e. failures);
- The number of time-steps in which the required temperature is reached in advance, since reaching the required comfort conditions some hours before the building is occupied would represent a loss of energy.

It is necessary to choose the algorithm parameters that gives the best trade-off between a low computational time and feasible accuracy (e.g. low predicted energy consumption, low energy loss).

Figure 4 represents the normalized energy consumption (with respect to the minimum) obtained for a single run of the DP algorithm with a prediction horizon of three days, for different values of  $\Delta u_1$  and  $\Delta u_2$ . Each plane refers to a different value of  $\Delta x$ . The figure shows that the influence of the input discretization on the global energy consumption is lower than the influence of the state discretization. In fact, the algorithm results in terms of energy consumption do not vary significantly for a given state grid step. Hence, it is possible to choose feasible values of the input grid steps and focus on the sensitivity analysis of the state grid step.

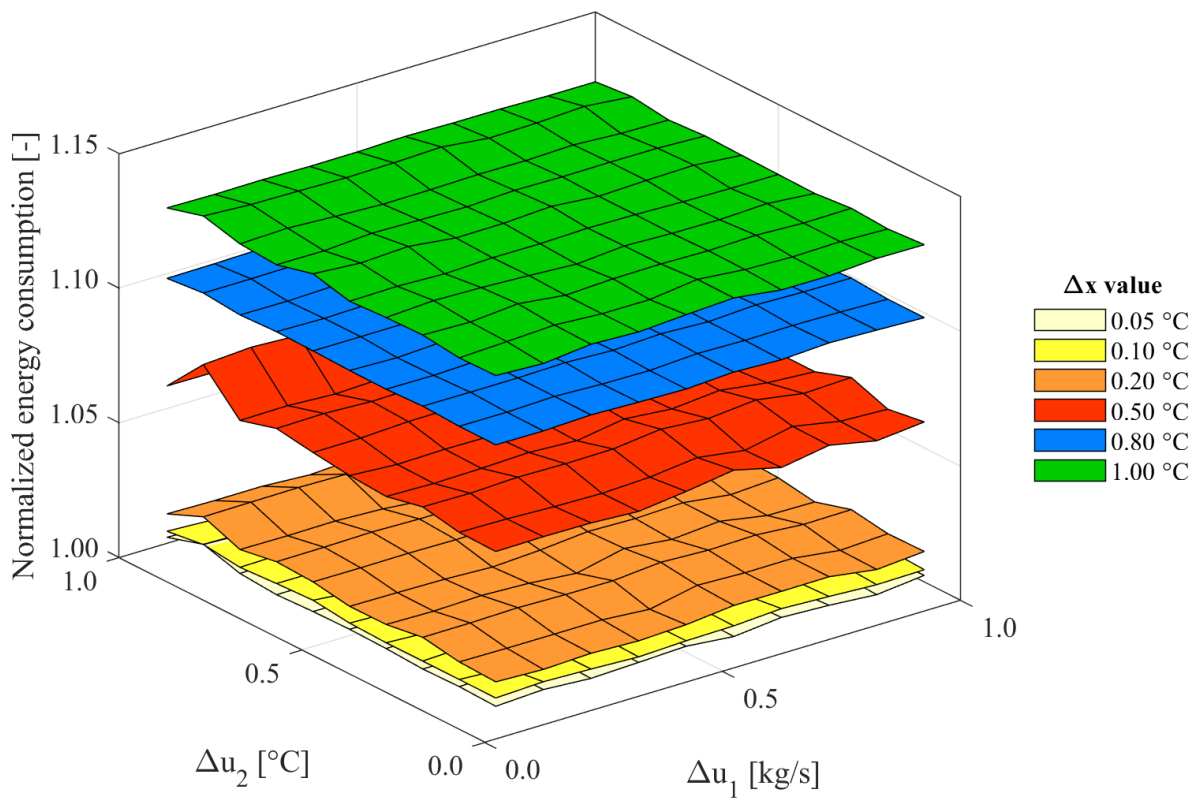


Figure 4. Predicted normalized energy consumption for different values of input grid steps. Each plane refers to a different value of the state grid step, from  $\Delta x = 0.05$  °C to  $\Delta x = 1$  °C.

Figure 5 represents the calculation time of one algorithm run for different input grid step settings. Since the computational time of an intermediate value of the input grid step can be considered acceptable for the online implementation of the MPC and, at the same time, the algorithm results are not significantly affected, it is reasonable to assume  $\Delta u_1 = 0.5$  kg/s and  $\Delta u_2 = 0.5$  °C to proceed with the analysis.

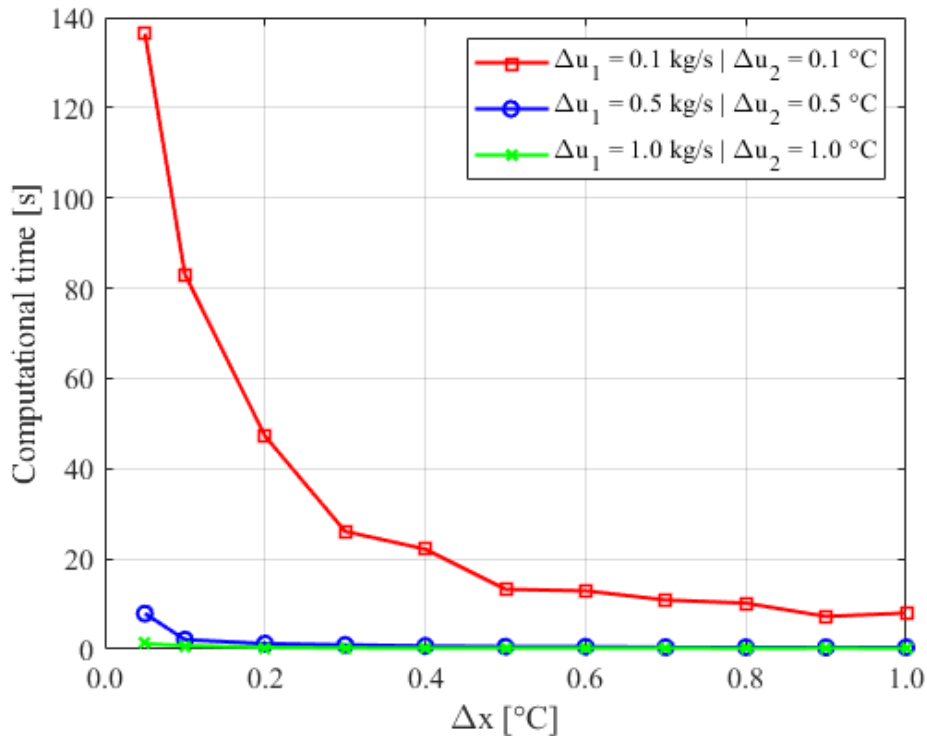
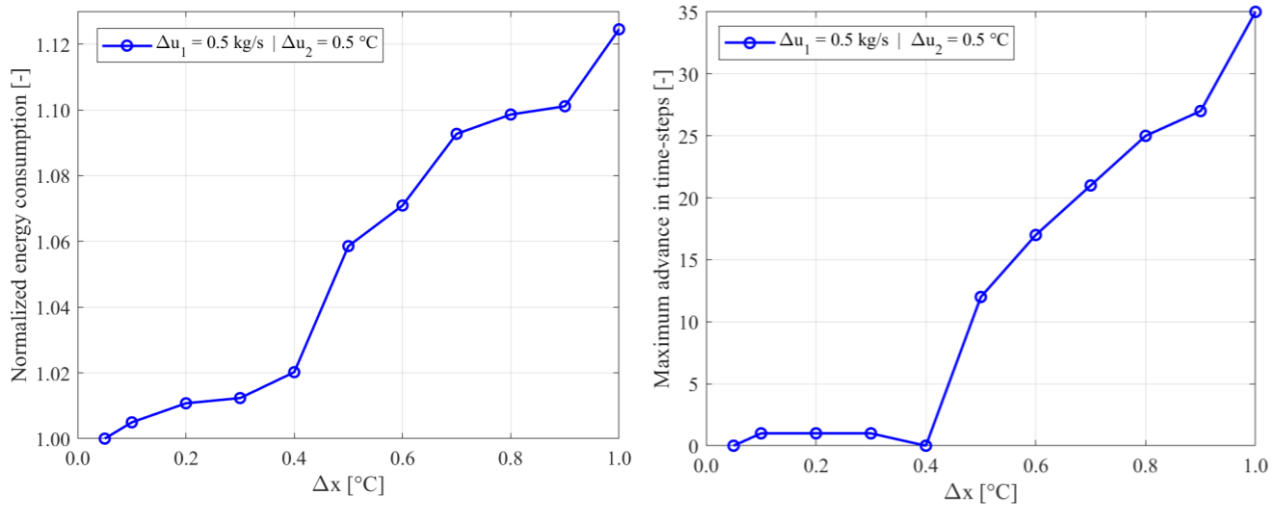


Figure 5. Computational time with varying state grid steps  $\Delta x$  for selected input grid step values  $\Delta u_1$  and  $\Delta u_2$ .

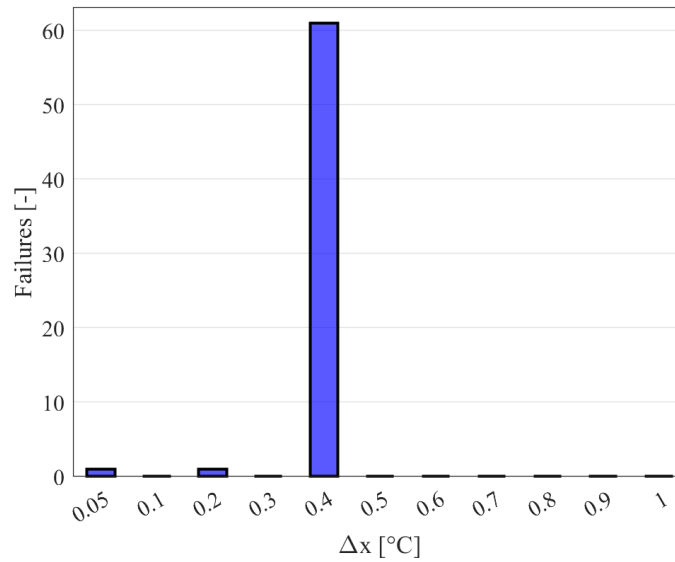
Figure 6 shows the variation of the last three key performance indicators (i.e. predicted global energy consumption, number of failures and number of time-steps in advance) with the state grid step  $\Delta x$ . The predicted energy consumption, normalized with respect to the minimum value obtained (Figure 6a), increases significantly with  $\Delta x$ . A finer state mesh allows the algorithm to evaluate the cost of each feasible state and select the optimal trajectory more precisely. As a matter of fact, linear interpolation is applied for the states between the grid points and this may lead to approximation uncertainties, since the state dependence on inputs and disturbances is not linear.

Furthermore, a lower value of  $\Delta x$  guarantees that internal building temperature requirements are satisfied (i.e. no failures) and the energy losses are minimized (i.e. temperature is not reached several hours before the building is occupied).



(a)

(b)



(c)

Figure 6. Results of the sensitivity analysis on the state grid step  $\Delta x$ : normalized predicted energy consumption (a), maximum advance of required temperature achievement in time-steps (b), number of time-steps in which the required temperature achievement fails (c). All results are obtained with  $\Delta u_1 = 0.5 \text{ kg/s}$  and  $\Delta u_2 = 0.5 \text{ }^{\circ}\text{C}$ .

A state grid step equal to  $0.4 \text{ }^{\circ}\text{C}$  leads to a large number of failures in the fulfillment of the required temperature for numerical reasons (Figure 6c). Indeed, that value results (i) in the comfort conditions being reached exactly at the requested time (i.e. maximum advance equal to zero) but also (ii) in the indoor temperature being maintained at a value which is slightly lower than the lower boundary during the maintenance phase. The algorithm returns optimal input values that are not able to keep

the state above the lower limit. This happens because the intrinsic discretization nature of the algorithm leads to the need to interpolate the values between the grid points, therefore producing numerical errors. In this case, the linear interpolation gives rise to the large number of failures corresponding to the state grid step of  $0.4\text{ }^{\circ}\text{C}$ . Higher values of  $\Delta x$ , on the other hand, allow the fulfillment of the required building conditions several time-steps (i.e. hours) before it is occupied with consequent energy waste (Figure 6b). Thus, it is possible to conclude that  $\Delta x$  values lower than  $0.4\text{ }^{\circ}\text{C}$  are acceptable for the accuracy of the algorithm and can therefore be considered for the MPC implementation.

This can be further confirmed by taking one building from the case study described in Section 5 as an example. Figure 7 represents the optimal behavior of the sports hall temperature as calculated by the algorithm with different values of  $\Delta x$ . By choosing a step equal to  $0.05\text{ }^{\circ}\text{C}$  or  $0.1\text{ }^{\circ}\text{C}$ , it is possible to keep the building temperature at around  $20\text{ }^{\circ}\text{C}$  only when required.

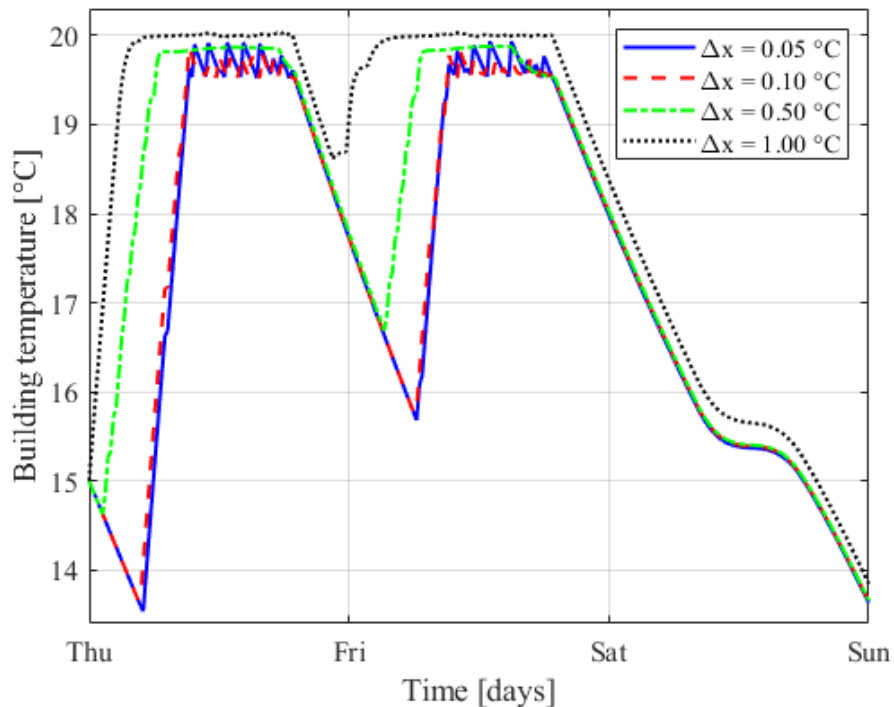


Figure 7. Optimal state (i.e. building temperature) trajectories over the prediction horizon calculated by one DP algorithm run with different state grid steps (sports hall).

## 5. Results and discussion

In this section, the MPC controller developed in Sections 3 and 4 is tested and compared to a state-of-the-art PID controller. In the conventional control approach, the water temperature is set at the maximum value and the PID regulates the water mass flow rate in order to reach the predefined set-point (i.e. building temperature).

After the description of the case study, the MPC-model is identified by means of simulation data and the results of the system MiL control are presented.

### 5.1 Case study description

The case study that was chosen to test this approach is a school complex in Northern Italy, depicted in Figure 8. A boiler supplies the thermal energy required by the sports hall and the school. A pipeline and a pump are dedicated to each building. The distribution pipes branch from the supply collector and, after supplying hot water to the buildings, go back to the return collector. The notation of the relevant sections of the pipes is referred to the MiL-model description in Section 3.2.

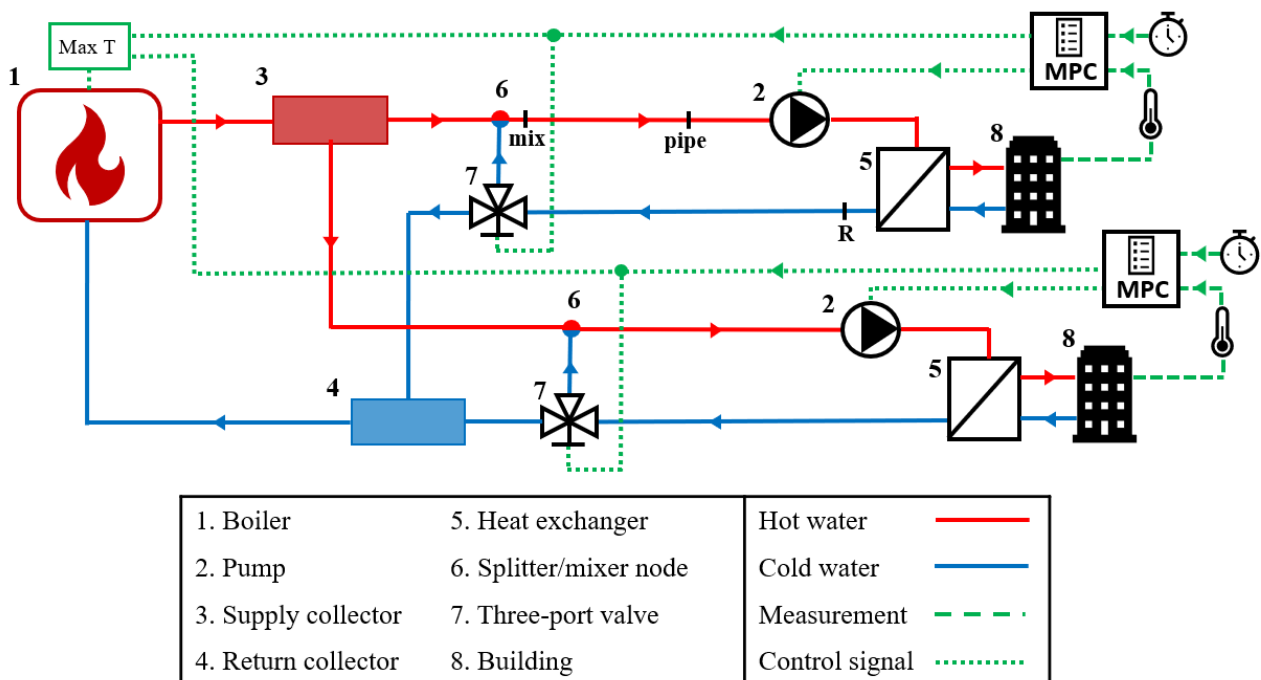


Figure 8. Schematic representation of the case study of the MPC control: a school complex located in Northern Italy. The underlined sections of the pipes are related to the model described in Section 3.2. **mix**: mixing; **pipe**: pipe; **R**: return.

As the MPC controller has been developed for a single-state system (e.g. a single building), a multi-agent approach is applied. Each branch of the system, characterized by a single building and dedicated distribution pipe, is controlled by its own MPC controller, which returns the optimal values of the water mass flow rate and supply temperature for the current time-step. The water mass flow rate is then regulated through the pump. As far as the supply temperature is concerned, the highest supply temperature returned by the MPC controllers is used to set the boiler. The actual water temperature of each building is then regulated by the mixing valve which recirculates part of the return cold water. Due to the internal temperature requirements, the lower and upper state constraints are assumed as 19.5 °C and 20.5 °C, respectively, when the building is occupied. The return water temperature has to be regulated by the substation heat exchanger controllers and its set-point  $T_{R,SP}$  is set to 60 °C. To this extent, the design temperature difference of the fluid in the secondary side of the heat exchanger  $\Delta T_{sec}$  is set to 10 °C. The relevant parameters of the case study described above are summarized in Table 1.

The multi-agent architecture allows this control approach to be extended to more complex networks by installing the MPC controller in the other branches of the system in a modular fashion.

### *5.2 Identification of the Model Predictive Control-model*

The MPC-model described in Section 3.1.1 has to be identified through the identification procedure. Identification is a methodology that builds the mathematical models of a system starting from input and output datasets.

In this application, these data are generated by running the MiL-model controlled by the PID for a simulation time of several days. The simulations make it possible to obtain sequences of (i) building internal temperature data, (ii) inputs defined by the PID and (iii) the imposed external temperature. These data are obtained with a sampling period of 15 minutes. Random components are added to both the internal and external temperatures to simulate measurement uncertainty. These data are divided into a training set for identification of the MPC-model parameters and a test set for validation.

Table 1. System parameters of the case study.

Parameter	Sports hall	School
Water mass flow rate	(0 to 8) kg/s	(0 to 12) kg/s
Supply temperature	(70 to 80) °C	(70 to 80) °C
Pipe length	100 m	50 m
Pipe diameter	100 mm	125 mm
Insulation thickness	100 mm	50 mm
Insulation conductivity	0.05 W/(m K)	0.05 W/(m K)
Friction factor	0.017	0.017
Pump efficiency	0.8	0.8
Number of occupants	50	400
Individual thermal power	120 W	80 W
Window surface	110 m <sup>2</sup>	100 m <sup>2</sup>
Coefficient $\tilde{a}$	$7.28 \cdot 10^{-6} \text{ s}^{-1}$	$3.50 \cdot 10^{-6} \text{ s}^{-1}$
Coefficient $\tilde{b}$	$7.53 \cdot 10^{-7} \text{ °C/kJ}$	$9.08 \cdot 10^{-7} \text{ °C/kJ}$
MPC prediction horizon	3 days	3 days
MPC time-step width	15 min	15 min

Parameter	Boiler
Nominal power	1700 kW
Minimum power	170 kW
Nominal efficiency	0.91
Minimum efficiency	0.85
<i>LHV</i> (natural gas)	47100 kJ/kg

The training set and the specified model structure are inputs of the identification problem. This consists of estimating the parameters of the model by solving a non-linear least-squares problem, which operates the minimization of the squared error between the model prediction and the dataset. By comparing the newly-identified gray-box model with the test set values, the reliability of the procedure can be evaluated. Once the MPC-model has been identified, it is possible to couple it with the DP optimization algorithm to constitute the predictive controller (Figure 2).

The set of real building input and output data is obtained by the simulation of fourteen days during the winter season. The test set is chosen as the last two days.

Figure 9 shows the temperature predicted by the model identified with two different training sets compared to the real temperature (i.e. original dataset) of the sports hall, which is taken as an example. The results highlight that the identification performed on a relatively short training set (e.g. 0.25 days) provides a model which does not adequately fit the measurements. This happens because the heating up and cooling down building dynamics are not sufficiently represented by the training set and cannot be highlighted.

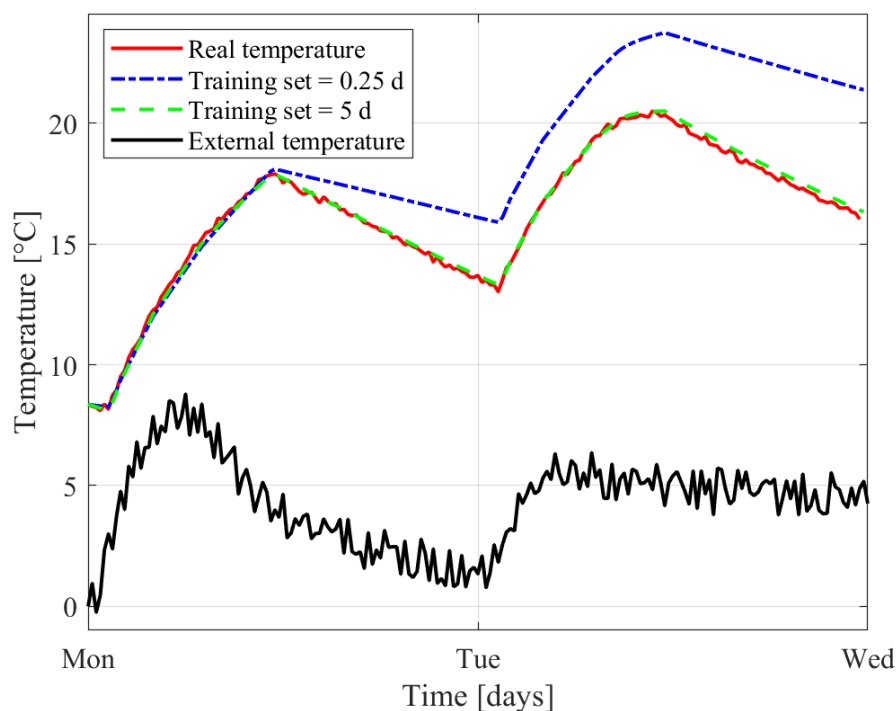


Figure 9. Comparison between identification results with two different training sets and real temperature data (sports hall).

Figure 10 shows the Root Mean Squared Error (RMSE) between predicted data and the measurements with varying training set lengths. Acceptable results are obtained with at least one-day-long datasets, provided that they cover typical weekday operation (i.e. with building heating and cooling transients). Similar conclusions can be drawn as far as the school is concerned.

The MPC-model building coefficients  $a$  and  $b$  chosen for controlling the sports hall and the school are obtained with training sets of five and six days, respectively, as they gave the lowest RMSE. The values of the coefficients are reported in Table 2.

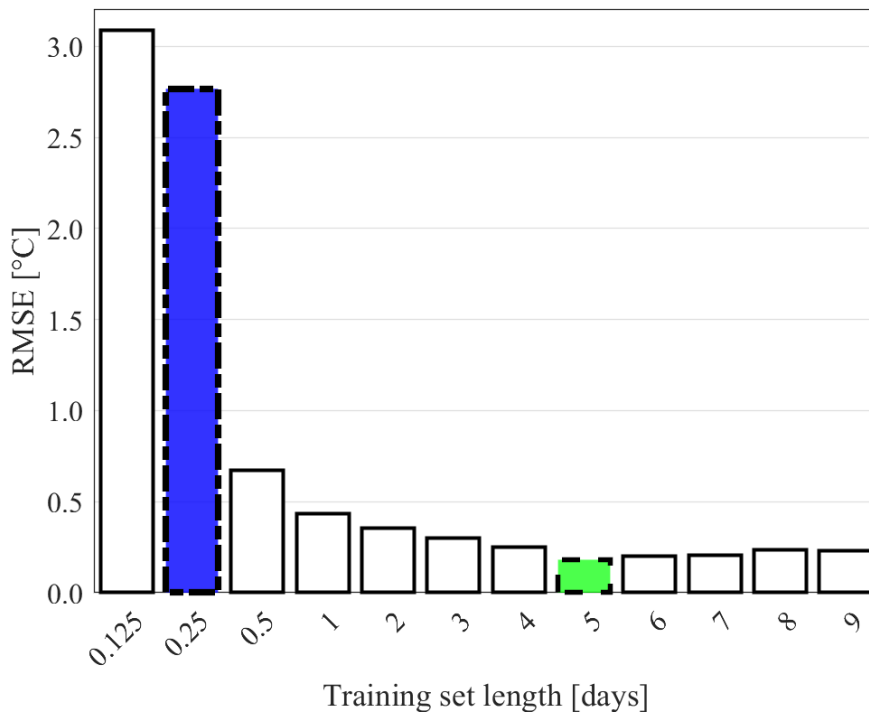


Figure 10. Root Mean Squared Error for different training set lengths (sports hall).

Table 2. MPC-model building performance coefficients obtained through the identification procedure.

Building	$a$ [ $s^{-1}$ ]	$b$ [ $^{\circ}C$ $kJ^{-1}$ ]
Sports hall	$6.9626 \cdot 10^{-6}$	$7.7983 \cdot 10^{-7}$
School	$2.9535 \cdot 10^{-6}$	$1.0719 \cdot 10^{-6}$

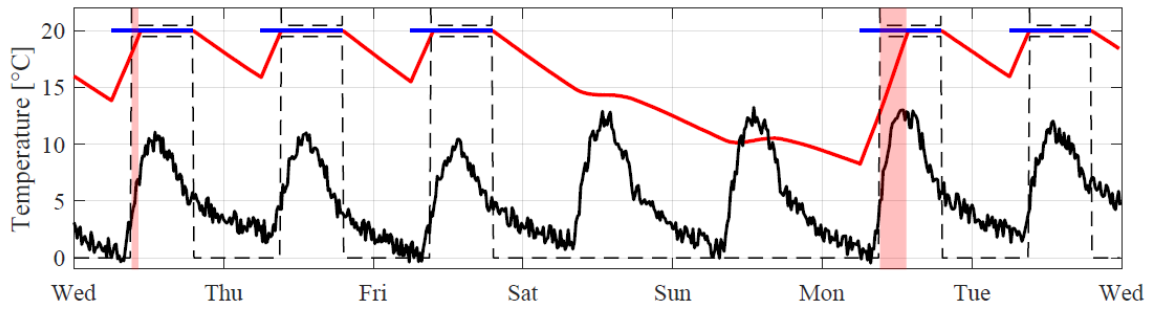
### 5.3 System control results and comparison

The system described in Section 5.1 is simulated for one week of the winter season through the MiL platform. The state-of-the-art PID controller and the MPC controller developed above are tested in the same conditions and the results are compared.

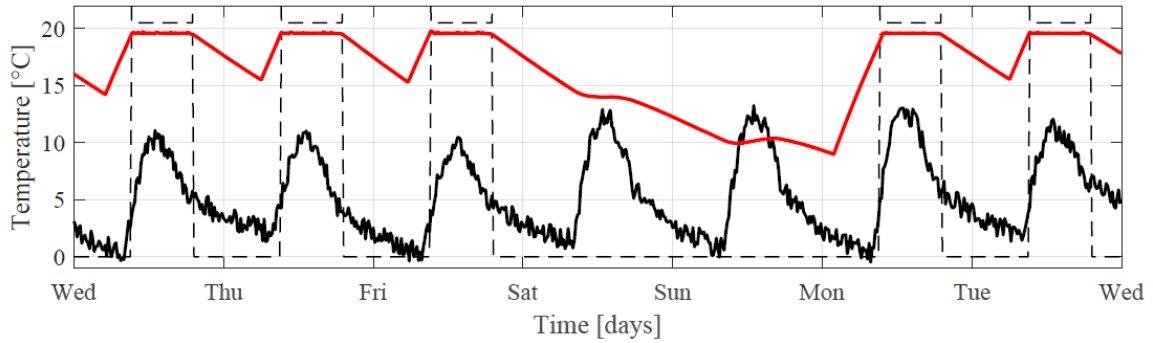
The model for the MPC controller implementation was identified in Section 5.2 while the optimization algorithm parameters were chosen through the sensitivity analysis in Section 4. The best trade-off between algorithm result accuracy and computational time is obtained by selecting  $\Delta u_1 = 0.5$  kg/s,  $\Delta u_2 = 0.5$  °C and  $\Delta x = 0.1$  °C. The prediction horizon of three days allows the dynamic behavior of the entire distribution network to be considered in the optimization, even when the weekend, or other days in which the buildings are not occupied, are involved. With these parameters, the DP algorithm calculation time is around 2 s with a standard laptop and, therefore, is suitable for the MPC controller online implementation for an energy network.

The comparison between the control performance of the PID and the MPC is shown in Figure 11 for the sports hall and Figure 12 for the school. It is possible to notice that the PID is not always able to guarantee the required internal temperature defined by the constraints (e.g. sports hall). Furthermore, in other conditions (e.g. school), the temperature is reached several hours before the building is actually occupied, causing non-necessary energy loss. Hence, this approach guarantees neither fulfillment of the desired comfort conditions nor energy minimization. This happens because a classical controller is based on a predefined rule and is not able to cope with the variation of the external conditions.

On the other hand, MPC assures compliance with the constraints while optimizing energy consumption. Moreover, MPC proves to be particularly effective with considerable variations in weather conditions that seem likely to happen due to climate change.



(a)



(b)

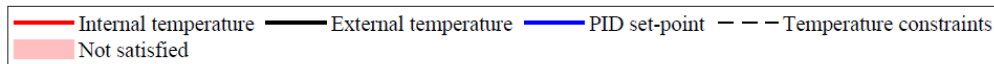
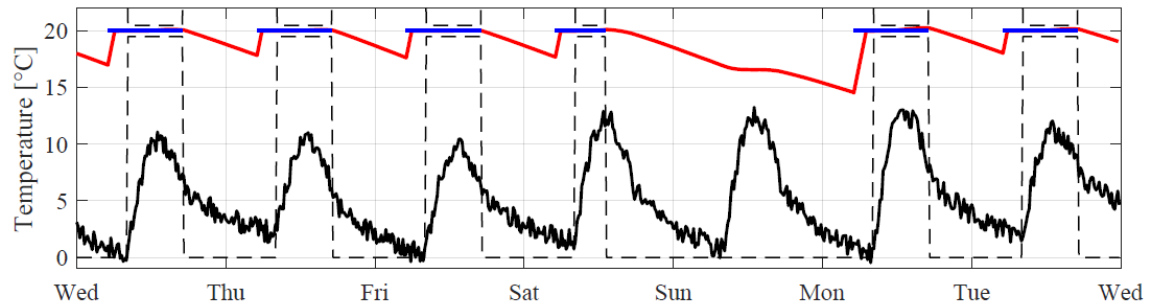
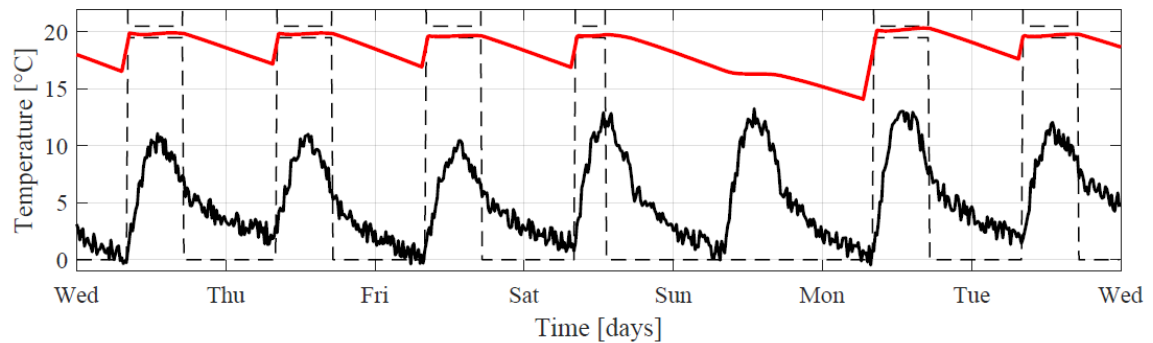


Figure 11. Model-in-the-Loop system operation of the sports hall with PID control (a) and MPC (b).



(a)



(b)

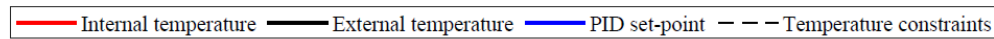
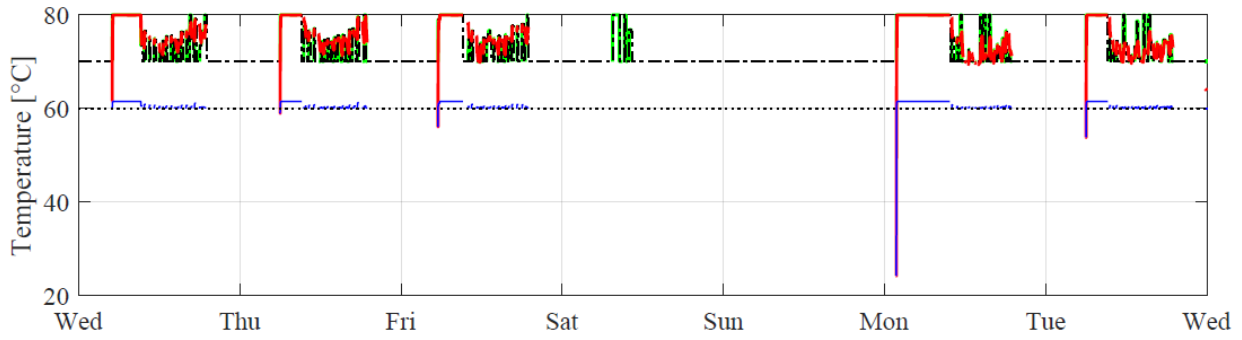


Figure 12. Model-in-the-Loop system operation of the school with PID control (a) and MPC (b).

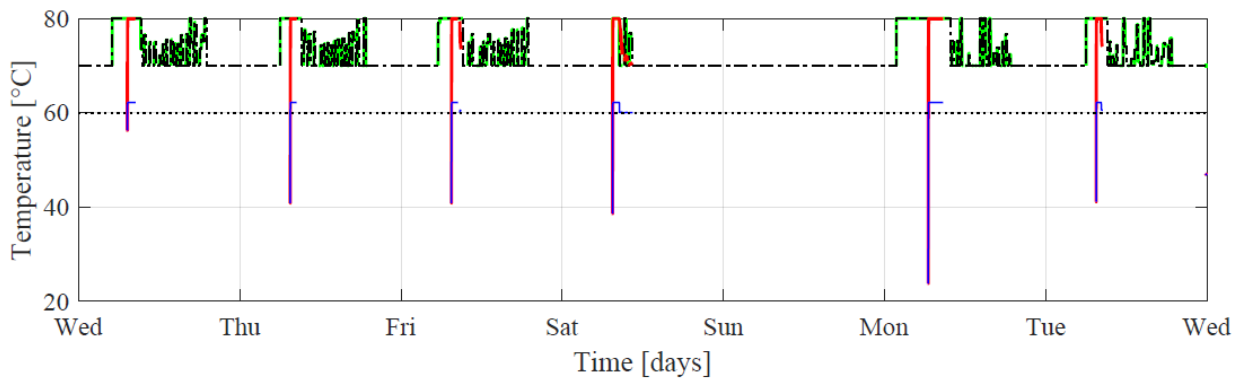
The two buildings behave differently due to the different values of the performance coefficients. The coefficient  $\tilde{a}$  affects the heat exchange through the walls while  $\tilde{b}$  influences the contribution of the thermal power transferred to the building. The higher the coefficient  $\tilde{a}$ , the greater the thermal loss to the outside. At the same time, the lower the coefficient  $\tilde{b}$ , the slower the heating process.

This is the case of the sports hall which, compared to the school, has a higher  $\tilde{a}$  and a lower  $\tilde{b}$  and, therefore, reaches a lower temperature when it is not occupied (i.e. cooling down process). Hence, the heating up of the sports hall has to start earlier than that of the school, especially after the weekend. The temperatures of the main water flows of the network are represented in Figure 13. In particular, the boiler temperature and return temperature track the set-points established by the MPC and set as a design parameter, respectively. Therefore, the assumption of the return temperature considered equal to the set-point parameter in the MPC-model is justified and produces reliable results. Moreover, the behavior of the pipe temperatures demonstrates the potential influence of the heat capacity of the water in the pipes. In the graph of each building (the sports hall in Figure 13a and the school in Figure 13b), the temperature values are not plotted when the related mass flow rate is equal to zero, since they lose significance. Nonetheless, it is possible to notice that the temperature of the water mass inside the pipes decreases due to the heat losses and the actual supply temperature to the substation heat exchanger is subjected to a heating transient. A more detailed pipe model might give a better insight into this phenomenon.

The supply temperatures as well as the related mass flow rates also vary according to the optimal inputs calculated by the controller. This is further noticed in Figure 14, which shows the water mass flow rate for both buildings during two representative days of the simulation. It is possible to state that, at the beginning of each day, the school requires only an initial maximum heating up, due to its higher heat capacity and maximum water mass flow rate. The sports hall, on the other hand, needs more water mass flow rate fluctuations in order to maintain the internal temperature. A predictive control method allows these results to be easily achieved.



(a)



(b)

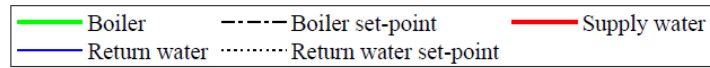


Figure 13. Temperatures of the water exiting the boiler and the supply and return water: (a) sports hall and (b) school.

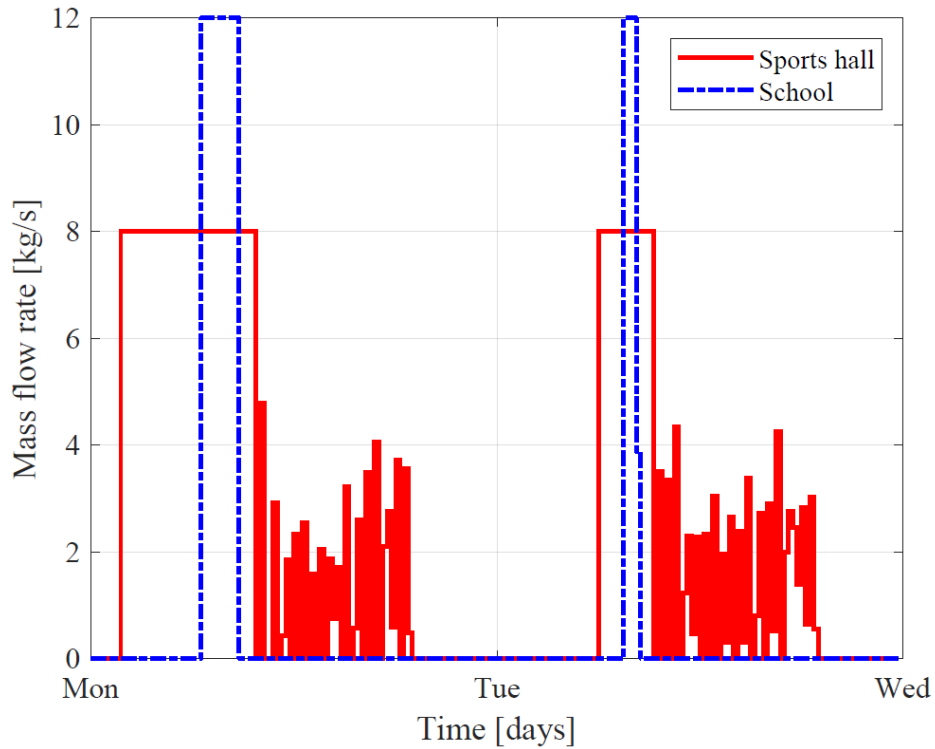


Figure 14. Mass flow rate of the water sent to the sports hall and the school during two representative days of the simulation.

As far as the primary energy consumption is concerned, the cumulated fuel mass used to power the boiler over the simulation horizon with the conventional controller and with the MPC controller is shown in Figure 15. In the latter case, a part of the fuel is saved until the weekend, during which the energy consumption of the conventional case is lower due to the fact that the building temperature required for the comfort of the occupants is not reached in time, as clarified by Figure 12. In the end, the fuel consumption is almost equal in the two cases, but the PID controller does not fulfill the constraints established by the contracts. This shows the superiority of the MPC controller and pledges a significant reduction in fuel consumption, when thermal comfort is kept.

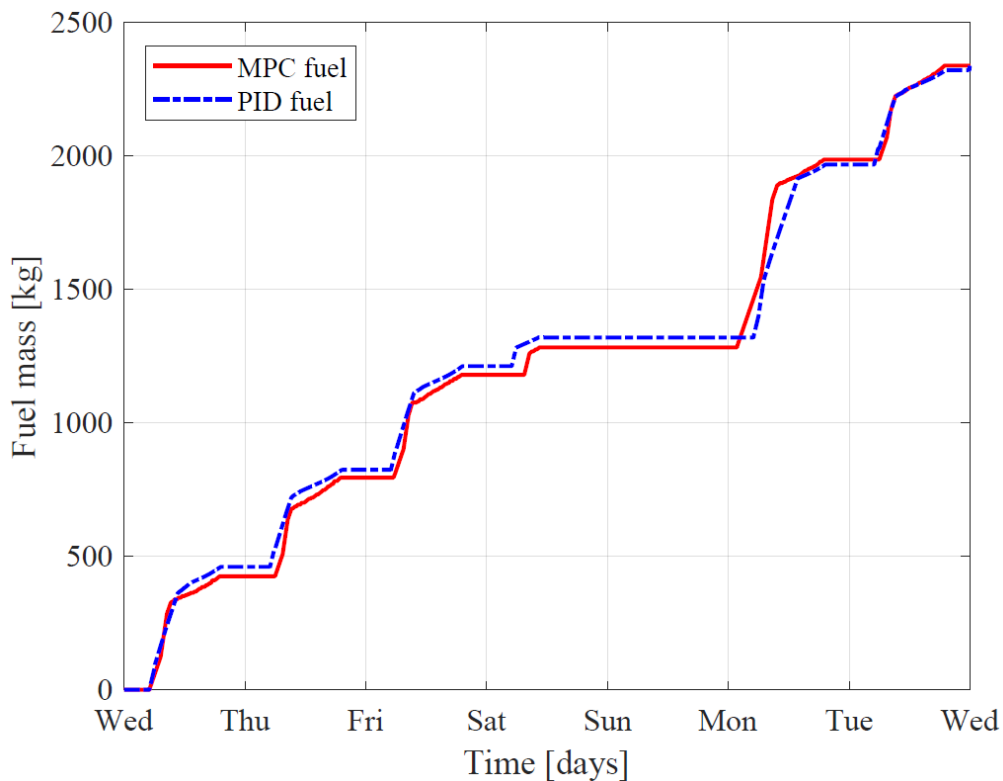


Figure 15. Cumulated fuel mass over the simulation period.

This primary energy saving is demonstrated in Table 3, which summarizes the results of the simulations for a week in January, a week in March and a week in November with different degrees of time advance for the activation of the PID set-points (the base case discussed above considers the activation three hours prior to the occupation of the buildings). For each case, the table reports (i) the percentage energy saving obtained with the MPC controller compared to the base case and (ii) the

failures (in hours) in meeting the internal temperature constraints that are avoided by using the MPC controller instead of the PID approach in the same conditions. It should be underlined that in some conditions the energy saving percentage is relatively low (e.g. week of January with three-hour time advance). However, as is clear from Table 3, this comes together with a significant time in which the constraint failures are avoided. For this reason, when the avoided failure time is higher than zero, the estimation of the energy saving percentage is conservative.

Hence, the MPC shows its ability to reduce the energy consumption while keeping the temperature constraints at different periods of the year with variable boundary conditions. This reduction is mainly due to two factors. Firstly, the MPC is able to convey to the end-users the necessary thermal energy exactly when it is needed, according to the boundary conditions. This is particularly convenient in DHCs, in which the characteristics of the connected buildings – and, therefore, the heating transients – are substantially diverse and a pre-defined rule is not able to consider this fact.

Table 3. Results of the primary energy saving obtained with the MPC controller compared to the PID controller (with different time schedules) in different simulations.

Simulation	PID time advance [h]	Energy saving [%]	Avoided failures [h]
January	3	0.32	5.25
	4	0.71	3.29
	5	2.56	2.44
March	3	2.21	4.17
	4	3.13	2.88
	5	4.81	1.88
November	3	4.55	1.22
	4	6.99	0
	5	7.28	0

Secondly, the MPC tends to maintain the building temperature close to the lower constraints avoiding unnecessary energy losses. If the lower value of the tolerance band (e.g. 19.5 °C) established as a hard constraint by the contract were applied as a set-point of the PID controller, those requirements would hardly be met due to the PID errors.

To conclude, the innovative MPC controller proposed in this work was tested with satisfactory results on two buildings of different types and at different distances from the heat production site. This opens up the possibility to further demonstrate the approach and extend these results to different buildings and larger systems.

## **6. Conclusions**

The current global energy scenario enables a significant reduction in energy consumption if efficiency in buildings and district heating and cooling networks is addressed.

In this work, a novel Model Predictive Controller based on a Dynamic Programming algorithm was developed and tested on a small-scale heat distribution network of a school complex in northern Italy through a Model-in-the-Loop platform. Firstly, detailed sensitivity analysis led to the selection of the most suitable parameters of the optimization algorithm. Secondly, the gray-box model embedded in the Model Predictive Controller was identified by means of an input-output dataset obtained by emulating the real system during the winter season. Another sensitivity analysis on the training set length made it possible to state that five-day-long datasets give acceptable fitting results. Subsequently, the operation of the district heating system was simulated in an Model-in-the-Loop to test the new controller and compare its results to those obtained with a classical PID controller. The system was controlled through a multi-agent approach by applying the Model Predictive Controller to each branch connected to a building in the network.

As expected, Model Predictive Control outperforms the PID with respect to both building comfort requirements and primary energy saving, regardless of the building type and the distribution pipe

length. Conservative results show a reduction in fuel consumption up to more than 7 %, depending on the season, obtained without altering the network configuration. For instance, in a week of January the energy saving is lower but this comes together with more than five hours of avoided failures of the comfort requirements compared to the conventional strategy. Hence, Model Predictive Control emerges as one of the most promising control strategies to be tackled in the attempt to reduce energy consumption and carbon emissions.

It should be remembered that the controller developed in this work represents an upper boundary for the control of these systems, since it assumes the ideal forecast of the external conditions. However, it can be extremely useful as a benchmark for comparison with other strategies. Moreover, robust control, which considers the uncertainties in the disturbance variables, is a potential future development. Further studies and applications of the proposed approach will focus on larger thermal networks. Lastly, future developments will concentrate on demonstrating how this innovative control approach can be implemented in real distribution networks.

## References

- [1] International Energy Agency official website. Energy Efficiency: Heating <https://www.iea.org/topics/energyefficiency/buildings/heating/> [accessed on 16/09/2019].
- [2] Lund H, Werner S, Wiltshire R, Svendsen S, Thorsen JE, Hvelplund F, Mathiesen BV. 4th Generation District Heating (4GDH) Integrating smart thermal grids into future sustainable energy systems. *Energy* 2014;68:1–11. <https://doi.org/10.1016/j.energy.2014.02.089>
- [3] Lake A, Rezaie B, Beyerlein S. Review of district heating and cooling systems for a sustainable future. *Renewable and Sustainable Energy Reviews* 2017;67:417–25. <https://doi.org/10.1016/j.rser.2016.09.061>
- [4] Li Y, Rezgui Y, Zhu H. District heating and cooling optimization and enhancement – Towards integration of renewables, storage and smart grid. *Renewable and Sustainable Energy Reviews* 2017;72:281–94. <https://doi.org/10.1016/j.rser.2017.01.061>
- [5] Clean energy for all Europeans. Publication Office of the European Union 2019. <https://doi.org/10.2833/21366>
- [6] Camacho EF, Bordons C. 1999. *Model Predictive Control*. Springer-Verlag London Limited. ISBN 3540762418.
- [7] Grüne L, Pannek J. 2011. *Nonlinear Model Predictive Control – Theory and Algorithms*. Springer-Verlag London Limited. ISBN 9780857295002.
- [8] Morari M, Lee JH. Model predictive control: past, present and future. *Computers and Chemical Engineering* 1999;23:667–682. [https://doi.org/10.1016/S0098-1354\(98\)00301-9](https://doi.org/10.1016/S0098-1354(98)00301-9)
- [9] Rawlings JB. Tutorial overview of model predictive control. *IEEE Control Systems Magazine* 2000;20:38–52. <https://doi.org/10.1109/37.845037>
- [10] Ellis M, Durand H, Christofides PD. A tutorial review of economic model predictive control methods. *Journal of Process Control* 2014;24:1156–78. <https://doi.org/10.1016/j.jprocont.2014.03.010>

- [11] Mayne DQ. Model predictive control: Recent developments and future promise. *Automatica* 2014;50:2967–86. <https://doi.org/10.1016/j.automatica.2014.10.128>
- [12] Heirung TAN, Paulson JA, O’Leary J, Mesbah A. Stochastic model predictive control – How does it work? *Computers and Chemical Engineering* 2018;114:158–70.  
<https://doi.org/10.1016/j.compchemeng.2017.10.026>
- [13] Crialesi Esposito M, Pompini N, Gambarotta A, Chandrasekaran V, Zhou J, Canova M. Nonlinear Model Predictive Control of an Organic Rankine Cycle for Exhaust Waste Heat Recovery in Automotive Engines. *IFAC-PapersOnLine* 2015;48:411–8.  
<https://doi.org/10.1016/j.ifacol.2015.10.059>
- [14] Liu X, Yebi A, Anshel P, Shetty J, Xu B, Hoffman M, Onori S. Model Predictive Control of an Organic Rankine Cycle System. *Energy Procedia* 2017;129:184–92.  
<https://doi.org/10.1016/j.egypro.2017.09.109>
- [15] Xu Q, Dubljevic S. Model predictive control of solar thermal system with borehole seasonal storage. *Computers and Chemical Engineering* 2017;101:59–72.  
<https://doi.org/10.1016/j.compchemeng.2017.02.023>
- [16] Rodrigues EMG, Godina R, Pouresmaeil E, Ferreira JR, Catalão JPS. Domestic appliances energy optimization with model predictive control. *Energy Conversion and Management* 2017;142:402–13. <https://doi.org/10.1016/j.enconman.2017.03.061>
- [17] Shafiei SE, Alleyne A. Model predictive control of hybrid thermal energy systems in transport refrigeration. *Applied Thermal Engineering* 2015;82:264–80.  
<https://doi.org/10.1016/j.applthermaleng.2015.02.053>
- [18] Zhang D, Huang X, Gao D, Cui X, Cai N. Experimental study on control performance comparison between model predictive control and proportion-integral-derivative control for radiant ceiling cooling integrated with underfloor ventilation system. *Applied Thermal Engineering* 2018;143:130–6. <https://doi.org/10.1016/j.applthermaleng.2018.07.046>

- [19] Shaikh P, Nor NBM, Nallagownden P, Elamvazuthi I, Ibrahim T. A review on optimized control systems for building energy and comfort management of smart sustainable buildings. *Renewable and Sustainable Energy Reviews* 2014;34:409–29.  
<https://doi.org/10.1016/j.rser.2014.03.027>
- [20] Li Y, Ang KH, Chong GCY. PID control system analysis and design. *IEEE Control Systems Magazine* 2006;26:32–41. <https://doi.org/10.1109/MCS.2006.1580152>
- [21] Prívvara S, Šíroký J, Ferkl L, Cigler J. Model predictive control of a building heating system: The first experience. *Energy and Buildings* 2011;43:564–72.  
<https://doi.org/10.1016/j.enbuild.2010.10.022>
- [22] Killian M, Kozek M. Ten questions concerning model predictive control for energy efficient buildings. *Building and Environment* 2016;105:403–12.  
<https://doi.org/10.1016/j.buildenv.2016.05.034>
- [23] Afram A, Janabi-Sharifi F. Theory and applications of HVAC control systems – A review of model predictive control (MPC). *Building and Environment* 2014;72:343–55.  
<https://doi.org/10.1016/j.buildenv.2013.11.016>
- [24] Clauß J, Finck C, Vogler-Finck P, Beagon P. Control strategies for building energy systems to unlock demand side flexibility – a review. *IBPSA Building Simulation Conference 2017*, San Francisco, USA, August 7–9, 2017. [http://www.ibpsa.org/proceedings/BS2017/BS2017\\_462.pdf](http://www.ibpsa.org/proceedings/BS2017/BS2017_462.pdf)
- [25] Bosschaerts W, Van Renterghem T, Hasan OA, Limam K. Development of a model based predictive control system for heating buildings. *Energy Procedia* 2017;112:519–28.  
<https://doi.org/10.1016/j.egypro.2017.03.1110>
- [26] Zong Y, Böning GM, Mirra Santos R, You S, Hu J, Han X. Challenges of implementing economic model predictive control strategy for buildings interacting with smart energy systems. *Applied Thermal Engineering* 2017;114:1476–86.  
<https://doi.org/10.1016/j.applthermaleng.2016.11.141>

[27] Prívará S, Cigler J, Váňa Z, Oldewurtel F, Sagerschnig C, Žáčková E. Building modeling as a crucial part for building predictive control. *Energy and Buildings* 2013;56:8–22.

<https://doi.org/10.1016/j.enbuild.2012.10.024>

[28] Ascione F, Bianco N, De Stasio C, Mauro GM, Vanoli GP. Simulation-based model predictive control by the multi-objective optimization of building energy performance and thermal comfort.

*Energy and Buildings* 2016;111:131–44. <https://doi.org/10.1016/j.enbuild.2015.11.033>

[29] Gholamibozanjani G, Tarragona J, de Gracia A, Fernández C, Cabeza LF, Farid MM. Model predictive control strategy applied to different types of building for space heating. *Applied Energy*

2018;231:959–71. <https://doi.org/10.1016/j.apenergy.2018.09.181>

[30] Salakij S, Yu N, Paolucci S, Antsaklis P. Model-Based Predictive Control for building energy management. I:Energy modeling and optimal control. *Energy and Buildings* 2016;133:345–58.

<https://doi.org/10.1016/j.enbuild.2016.09.044>

[31] Johansson C, Bergkvist M, Geysen D, De Somer O, Lavesson N, Vanhoudt D. Operational Demand Forecasting In District Heating Systems Using Ensembles Of Online Machine Learning

Algorithms. *Energy Procedia* 2017;116:201-216. <https://doi.org/10.1016/j.egypro.2017.05.068>

[32] Reynolds J, Rezgui Y, Kwan A, Piriou S. A zone-level, building energy optimisation combining an artificial neural network, a genetic algorithm, and model predictive control. *Energy*

2018;151:729–39. <https://doi.org/10.1016/j.energy.2018.03.113>

[33] Bianchini G, Casini M, Pepe D, Vicino A, Zanvettor GG. An integrated model predictive control approach for optimal HVAC and energy storage operation in large-scale buildings. *Applied*

*Energy* 2019;240:327–40. <https://doi.org/10.1016/j.apenergy.2019.01.187>

[34] Sangi R, Kümpel A, Müller D. Real-life implementation of a linear model predictive control in a building energy system. *Journal of Building Engineering* 2019;22:451–63.

<https://doi.org/10.1016/j.jobbe.2019.01.002>

- [35] Fux SF, Benz MJ, Guzzella L. Economic and environmental aspects of the component sizing for a stand-alone building energy system: A case study. *Renewable Energy* 2013;55:438–47. <https://doi.org/10.1016/j.renene.2012.12.034>
- [36] Kuboth S, Heberle F, König-Haagen A, Brüggemann D. Economic model predictive control of combined thermal and electric residential building energy systems. *Applied Energy* 2019;240:372–85. <https://doi.org/10.1016/j.apenergy.2019.01.097>
- [37] Parisio A, Rikos E, Glielmo L. A Model Predictive Control Approach to Microgrid Operation Optimization. *IEEE Transactions on Control Systems Technology* 2014;22:1813-1827. <https://doi.org/10.1109/TCST.2013.2295737>
- [38] Sultana WR, Sahoo SK, Sukchai S, Yamuna S, Venkatesh D. A review on state of art development of model predictive control for renewable energy applications. *Renewable and Sustainable Energy Reviews* 2017;76:391-406. <https://doi.org/10.1016/j.rser.2017.03.058>
- [39] Vandermeulen A, Van der Heijde B, Helsen L. Controlling district heating and cooling networks to unlock flexibility: A review. *Energy* 2018;151:103-115. <https://doi.org/10.1016/j.energy.2018.03.034>
- [40] Verrilli F, Srinivasan S, Gambino G, Canelli M, Himanka M, Del Vecchio C, Sasso M, Glielmo L. Model Predictive Control-Based Optimal Operations of District Heating System With Thermal Energy Storage and Flexible Loads. *IEEE Transactions on Automation Science and Engineering* 2017;14:547-557. <https://doi.org/10.1109/TASE.2016.2618948>
- [41] Vanhoudt D, Claessens BJ, Salenbien R, Desmedt J. An active control strategy for district heating networks and the effect of different thermal energy storage configurations. *Energy and Buildings* 2018;158:1317–27. <https://doi.org/10.1016/j.enbuild.2017.11.018>
- [42] Lennermo G, Lauenburg P, Werner S. Control of decentralised solar district heating. *Solar Energy* 2019;179:307–15. <https://doi.org/10.1016/j.solener.2018.12.080>

- [43] Long S, Marjanovic O, Parisio A. Generalised control-oriented modelling framework for multi-energy systems. *Applied Energy* 2019;235:320–31.  
<https://doi.org/10.1016/j.apenergy.2018.10.074>
- [44] Dounis AI, Caraiscos C. Advanced control systems engineering for energy and comfort management in a building environment—A review. *Renewable and Sustainable Energy Reviews* 2009;13:1246-1261. <https://doi.org/10.1016/j.rser.2008.09.015>
- [45] Sameti M, Haghghat F. Optimization approaches in district heating and cooling thermal network. *Energy and Buildings* 2017;140:121–30. <https://doi.org/10.1016/j.enbuild.2017.01.062>
- [46] Kuang J, Zhang C, Sun B. Stochastic dynamic solution for off-design operation optimization of combined cooling, heating, and power systems with energy storage. *Applied Thermal Engineering* 2019;160:113967. <https://doi.org/10.1016/j.applthermaleng.2019.114356>
- [47] Bahlawan H, Morini M, Pinelli M, Spina PR. Dynamic programming based methodology for the optimization of the sizing and operation of hybrid energy plants. *Applied Thermal Engineering* 2019;160:113967. <https://doi.org/10.1016/j.applthermaleng.2019.113967>
- [48] Favre B, Peuportier B. Application of dynamic programming to study load shifting in buildings. *Energy and Buildings* 2014;82:57–64. <https://doi.org/10.1016/j.enbuild.2014.07.018>
- [49] Guelpa E, Marincioni L, Capone M, Deputato S, Verda V. Thermal load prediction district in district heating systems. *Energy* 2019;176:693–703. <https://doi.org/10.1016/j.energy.2019.04.021>
- [50] Hammer A, Sejkora C, Kienberger T. Increasing district heating networks efficiency by means of temperature-flexible operation. *Sustainable Energy, Grids and Networks* 2018;16:393–404.  
<https://doi.org/10.1016/j.segan.2018.11.001>
- [51] Guelpa E, Deputato S, Verda V. Thermal request optimization in district heating networks using a clustering approach. *Applied Energy* 2018;228:608–17.  
<https://doi.org/10.1016/j.apenergy.2018.06.041>
- [52] Li X, Wen J. Review of building energy modeling for control and operation. *Renewable and Sustainable Energy Reviews* 2014; 37:517-537. <https://doi.org/10.1016/j.rser.2014.05.056>

- [53] Gambarotta A, Morini M, Rossi M, Stonfer M. A library for the simulation of smart energy systems: the case of the Campus of the University of Parma. *Energy Procedia* 2017;105:1776–81.  
<https://doi.org/10.1016/j.egypro.2017.03.514>
- [54] Cesaraccio C, Spano D, Duce P, Snyder RL. An improved model for determining degree-day values from daily temperature data. *International Journal of Biometeorology* 2001;45:161–9.  
<https://doi.org/10.1007/s004840100104>
- [55] Sundström O, Guzzella L. A Generic Dynamic Programming Matlab Function. *Control Applications, (CCA) & Intelligent Control, (ISIC), 2009 IEEE*, pp.1625-30, 8-10 July 2009.  
<https://doi.org/10.1109/CCA.2009.5281131>
- [56] Dainese C, Faè M, Gambarotta A, Morini M, Premoli M, Randazzo G, Rossi M, Rovati M, Saletti C. Development and application of a Predictive Controller to a mini district heating network fed by a biomass boiler. *Energy Procedia* 2019;159:48-53.  
<https://doi.org/10.1016/j.egypro.2018.12.016>
- [57] Van der Heijde B, Fuchs M, Ribas Tugores C, Schweiger G, Sartor K, Basciotti D, Müller D, Nytsch-Geusen C, Wetter M, Helsen L. Dynamic equation-based thermo-hydraulic pipe model for district heating and cooling systems. *Energy Conversion and Management* 2017;151:158-169.  
<https://doi.org/10.1016/j.enconman.2017.08.072>
- [58] Dénarié A, Aprile M, Motta M. Heat transmission over long pipes: New model for fast and accurate district heating simulations. *Energy* 2019;166:267-276.  
<https://doi.org/10.1016/j.energy.2018.09.186>

## Nomenclature

$a$	first building performance coefficient [ $s^{-1}$ ]
$b$	second building performance coefficient [ $^{\circ}C\ kJ^{-1}$ ]
$c$	water specific heat capacity [ $kJ\ kg^{-1}\ K^{-1}$ ]
$cost$	cost function [kJ]
$d$	system disturbance
$D$	pipe diameter [m]
$f$	pipe friction factor [-]
$K_p$	coefficient of proportionality of the controller
$k$	coefficient of proportionality of the pump power [ $m^2\ kg^{-2}$ ]
$L$	pipe length [m]
$LHV$	fuel lower heating value [ $kJ\ kg^{-1}$ ]
$M$	water mass inside the pipe [kg]
$\dot{m}$	water mass flow rate [ $kg\ s^{-1}$ ]
$P$	power [kW]
$\dot{Q}$	thermal power [kW]
$T$	temperature [ $^{\circ}C$ ]
$t$	time [s]
$u$	system input
UA	overall heat transfer coefficient [ $kW\ K^{-1}$ ]

$\Delta t$	time-step [s]
$\Delta t_d$	time delay factor [s]
$x$	system state
$\eta$	efficiency [-]
$\rho$	water density [ $\text{kg m}^{-3}$ ]
$\varphi$	penalty cost factor for constraint violation [kJ]

*Subscripts*

boiler	boiler
DP	Dynamic Programming optimal input
ext	external
f	fuel
irr	irradiance
k	number of time-step
loss	loss
min	minimum
mix	mixing
new	new input
nom	nominal
occ	building occupation
pipe	pipe

previous	input at previous time-step
pump	pump
R	return
rec	recirculated
S	supply
sec	secondary side of the building substation heat exchanger
soil	soil
SP	set-point

*Acronyms*

DHC	District Heating and Cooling
DP	Dynamic Programming
EU	European Union
HVAC	Heating Ventilation and Air Conditioning
MiL	Model-in-the-Loop
MILP	Mixed Integer Linear Programming
MPC	Model Predictive Control
PID	Proportional-Integral-Derivative controller
RMSE	Root Mean Squared Error

## List of figures

Figure 1. Schematic representation of the concept of Model Predictive Control.

Figure 2. Block diagram of the method for the development of the innovative controller.

Figure 3. Schematic representation of the distribution pipeline for each building.

Figure 4. Predicted normalized energy consumption for different values of input grid steps.

Figure 5. Computational time with varying state grid steps  $\Delta x$  for selected input grid step values  $\Delta u_1$  and  $\Delta u_2$ .

Figure 6. Results of the sensitivity analysis on the state grid step  $\Delta x$ : normalized predicted energy consumption (a), maximum advance of required temperature achievement in time-steps (b), number of time-steps in which the required temperature achievement fails (c).

Figure 7. Optimal state (i.e. building temperature) trajectories over the prediction horizon calculated by one DP algorithm run with different state grid steps (sports hall).

Figure 8. Schematic representation of the case study of the MPC control: a school complex located in Northern Italy.

Figure 9. Comparison between identification results with two different training sets and real temperature data (sports hall).

Figure 10. Root Mean Squared Error for different training set lengths (sports hall).

Figure 11. Model-in-the-Loop system operation of the sports hall with PID control (a) and MPC (b).

Figure 12. Model-in-the-Loop system operation of the school with PID control (a) and MPC (b).

Figure 13. Temperatures of the water exiting the boiler and the supply and return water: (a) sports hall and (b) school.

Figure 14. Mass flow rate of the water sent to the sports hall and the school during two representative days of the simulation.

Figure 15. Cumulated fuel mass over the simulation period.

## **List of tables**

Table 1. System parameters of the case study.

Table 2. MPC-model building performance coefficients obtained through the identification procedure.

Table 3. Results of the primary energy saving obtained with the MPC controller compared to the PID controller (with different time schedules) in different simulations.